

## Organ and effective dose conversion coefficients for a sitting female hybrid computational phantom exposed to monoenergetic protons in idealized irradiation geometries

This content has been downloaded from IOPscience. Please scroll down to see the full text.

2014 Phys. Med. Biol. 59 7957

(<http://iopscience.iop.org/0031-9155/59/24/7957>)

View the [table of contents for this issue](#), or go to the [journal homepage](#) for more

Download details:

IP Address: 143.107.255.190

This content was downloaded on 15/07/2015 at 11:53

Please note that [terms and conditions apply](#).

# Organ and effective dose conversion coefficients for a sitting female hybrid computational phantom exposed to monoenergetic protons in idealized irradiation geometries

M C Alves<sup>1</sup>, W S Santos<sup>2</sup>, Choonsik Lee<sup>3</sup>, Wesley E Bolch<sup>4</sup>,  
John G Hunt<sup>5</sup> and A B Carvalho Júnior<sup>1</sup>

<sup>1</sup> Departamento de Física, Universidade Federal de Sergipe, Campus Prof. José Aloísio de Campos, 49.100-000, São Cristóvão—SE, Brazil

<sup>2</sup> Instituto de Pesquisas Energéticas e Nucleares, Comissão Nacional de Energia Nuclear (IPEN/CNEN/SP) São Paulo, Brazil

<sup>3</sup> Division of Cancer Epidemiology and Genetics, National Cancer Institute, National Institute of Health, Bethesda, MD 20852, USA

<sup>4</sup> Department of Nuclear and Radiological Engineering, University of Florida, Gainesville, FL 32611–8300, USA

<sup>5</sup> Dosimetry Division, Instituto de Radioproteção e Dosimetria, Rio de Janeiro, RJ 22783-127, Brazil

E-mail: [alves.materia@gmail.com](mailto:alves.materia@gmail.com)

Received 28 July 2014, revised 23 September 2014

Accepted for publication 24 October 2014

Published 26 November 2014

## Abstract

The conversion coefficients (CCs) relate protection quantities, mean absorbed dose ( $D_T$ ) and effective dose ( $E$ ), with physical radiation field quantities, such as fluence ( $\Phi$ ). The calculation of CCs through Monte Carlo simulations is useful for estimating the dose in individuals exposed to radiation. The aim of this work was the calculation of conversion coefficients for absorbed and effective doses per fluence ( $D_T/\Phi$  and  $E/\Phi$ ) using a sitting and standing female hybrid phantom (UFH/NCI) exposure to monoenergetic protons with energy ranging from 2 MeV to 10 GeV. The radiation transport code MCNPX was used to develop exposure scenarios implementing the female UFH/NCI phantom in sitting and standing postures. Whole-body irradiations were performed using the recommended irradiation geometries by ICRP publication 116 (AP, PA, RLAT, LLAT, ROT and ISO). In most organs, the conversion coefficients  $D_T/\Phi$  were similar for both postures. However, relative differences were significant for organs located in the abdominal region, such as ovaries, uterus and urinary bladder, especially

in the AP, RLAT and LLAT geometries. Anatomical differences caused by changing the posture of the female UFH/NCI phantom led an attenuation of incident protons with energies below 150 MeV by the thigh of the phantom in the sitting posture, for the front-to-back irradiation, and by the arms and hands of the phantom in the standing posture, for the lateral irradiation.

Keywords: protons, computational dosimetry, conversion coefficients

(Some figures may appear in colour only in the online journal)

## 1. Introduction

Background radiation is mainly formed by cosmic radiation, in which nearly 90% are energetic protons (Townsend 2001). Secondary radiations such as protons, neutrons, pion and muons are produced when cosmic radiation penetrates the atmosphere causing nuclear reactions with its constituents (Reitz 1993). Estimating the dose due occupational exposures to this type of radiation is important, including workers such as aircraft crew, who are normally exposed to a significant amount of proton beams.

Due to the difficulty in estimating the absorbed dose in an individual through experimental techniques, computational human phantom coupled to Monte Carlo radiation transport code can simulate exposure scenarios to estimate the absorbed dose in organ or tissue. The simulation technique provides dose conversion coefficients, which converts measured quantity (e.g. air kerma) to absorbed dose (ICRP 2010). Monte Carlo method is a widespread technique that uses probability density functions and random numbers in order to determine energy, position, direction and path-length of individual particles as well the type of physical interaction that occurs when radiation interacts with matter (Bozkurt and Xu 2004). Computational human phantoms are computational representations of the human anatomy (Kramer *et al* 2004). To date, two classes of computational phantoms have been used in computational dosimetry: Constructive Solid Geometry (CSG) and Boundary Representation (BREP) phantoms. Examples of CSG are the mathematical and voxel phantoms (Xu 2010). In mathematical phantoms, anatomical structures are represented by mathematical equations such as planes, cylinders, spheres and cones. Voxel phantoms are constructed from medical images (computed tomography or magnetic resonance imaging) of real patients or from the sectional color photographs of cadaver. Although voxel phantoms provide more realistic anatomical representation for dosimetry calculations, there are some limitations such as the dependence of organs contour with images segmentation and the individual anatomy reflecting the tomographic data. To overcome these limitations and with the advance of computer graphics, BREP phantoms were introduced more recently which take advantage of the realistic anatomy of voxel phantoms and the flexibility of mathematical phantoms for adjusting organ contours and volumes. Hybrid phantoms, which belongs to the BREP class of phantoms, are developed basically from medical images, like voxel phantom, but three steps is performed: polygonization of voxel phantom, modelling internal organ structure via polygon mesh and NURBS (non-uniform rational B-spline) surface to match reference organ volumes and phantom voxelization (Piegls 1991, Lee 2007).

Several researchers used voxel phantoms for the calculation of dose conversion coefficients for protons (Bozkurt and Xu 2004, Zhang 2008, Sato 2009). However, no studies using computational phantoms in sitting posture have been reported. Dosimetric calculations suggest that for external exposures, specifically the posture may influence the absorbed doses in

organs significantly. Thus, use phantoms with variable stature in standing or sitting, depending on the scenario of irradiation, is another step to make the simulation of increasingly specific exposure, e.g. airplane crew. The problem, strictly speaking, is that the results can only be applied to a person who has the same posture of the phantom, while for a person with different posture, values can be wrong. To better represent these posture differences, this study presents adult anthropomorphic phantoms, in both standing and sitting developed for the calculation of absorbed doses in radiosensitive organs and tissues of the human body. The aims of the current study were calculate absorbed and effective dose conversion coefficients using a standing and a sitting adult female hybrid simulator exposure to monoenergetic protons in antero-posterior (AP), postero-anterior (PA), right-lateral (RLAT), left-lateral (LLAT), rotational (ROT) and isotropic (ISO) geometries. The conversion factors from different postures were compared to each other.

## 2. Materials and methods

### 2.1. Monte Carlo code

In this work, simulations were performed using the MCNPX code (Version 2.7), a general purpose Monte Carlo transport code developed from the Los Alamos National Laboratory (LANL) (Pelowitz 2011). The code can handle the 3D geometry transport and interaction of neutrons, protons, electrons, photons, heavy charged particles and others in a wide range of energies (Briesmeister 2000). MCNPX was used for simulating proton interactions and secondary particles (photons, electrons, neutrons, other protons) generated when protons interact with matter. In order to model the interactions of thermal neutrons with the molecules in the body, the  $S(\alpha,\beta)$  function describing the scattering law for light water molecules at 300K temperature was employed for all materials of organs and tissues. This model was considered necessary in all simulations since a typical proton interaction will produce neutrons which tend to be down-scattered to thermal energies (Briesmeister 1997).

### 2.2. Hybrid computational phantom

The Hybrid Adult Female computational human phantom developed at the University of Florida and the National Cancer Institute (Lee 2010) (figure 1) was implemented in MCNPX code in two postures: standing and sitting. The legs including skeletal structures of the original hybrid phantom in NURBS-format were deformed to represent the same phantom in sitting posture. Multiple control points included in the surface of legs and skeletons were adjusted using a 3D modeling software, Rhinoceros. Modification to other body parts except legs was not attempted.

### 2.3. Exposure scenarios

Exposure scenarios were developed for the two phantoms in different postures independently. In both postures, the phantom, surrounded by vacuum, was irradiated by monoenergetic protons with the energies from 2 MeV to 10 GeV in six irradiation geometries: antero-posterior (AP), postero-anterior (PA), right-lateral (RLAT), left-lateral (LLAT), rotational (ROT) and isotropic (ISO), which are defined in the ICRP Publication 116 [3]. In each simulation  $10^8$  particle histories were considered in order to keep the relative error under 10% in all organs of interest. Values of energy deposited by all particles transported

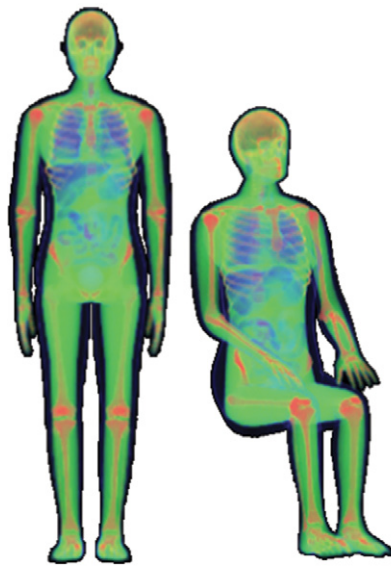


**Figure 1.** 3D renderings of the UFH/NCI adult female hybrid phantoms in the standing (left) and sitting (right) postures.

in the simulations were normalized by incident proton fluence to derive organ dose conversion coefficients ( $\text{pGy cm}^2$ ). The organ dose conversion coefficients ( $D_T/\Phi$ ) and effective dose conversion coefficients ( $E/\Phi$ ) of the standing and sitting UFH/NCI adult female phantoms were calculated and compared to each other. The F6 tally command of MCNPX was used to calculate absorbed dose in organs and tissues for protons and secondary particles generated. To obtain the equivalent-dose conversion coefficients, the organ-dose conversion coefficients were multiplied by 2, which is the radiation weighting factor of protons, as recommended in ICRP Publication 103 (2007). Red bone marrow (RBM) and bone surface are not explicitly defined in the hybrid phantoms since these tissues are presented in sophisticated spongiosa and medullary cavity structures. Therefore, the absorbed dose in RBM was determined by averaging the absorbed dose in each spongiosa multiplied with the mass ratios of red bone marrow contained in each region (ICRP 2010). The absorbed dose in bone surface was obtained from the absorbed dose in each spongiosa and medullary cavity, which contain endosteum tissue, multiplied with the mass ratios of endosteum contained in each region (ICRP 2010).

### 3. Results and discussion

Initially, results of fluence-to-absorbed dose conversion coefficients of the UFH/NCI female phantom in the standing posture were compared with the ICRP female phantom in AP, PA, RLAT and ISO irradiation geometries (ICRP 2007, 2010). The comparison of fluence-to-absorbed dose conversion coefficients for four representative organs (breast, red bone marrow, skin and uterus) are presented in attached tables A.1–A.4. As presented in tables A.1–A.4, high relative differences were observed between conversion coefficients of the UFH/NCI and the ICRP phantom in energies lower than 100 MeV. In skin, for example, conversion coefficients of ICRP female phantom are until 45% higher than

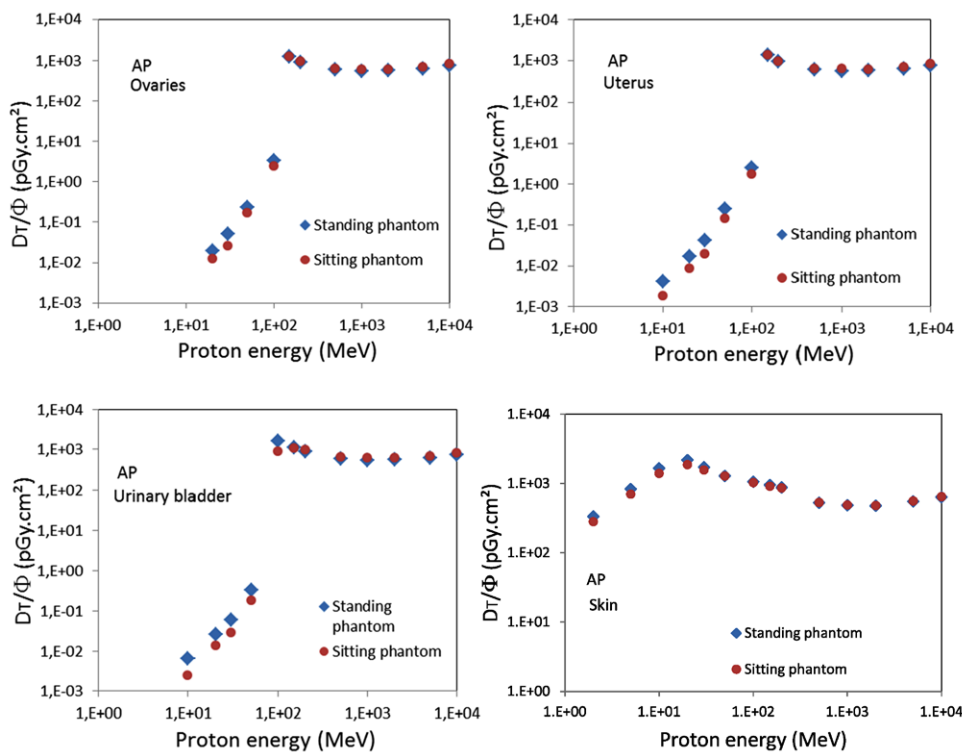


**Figure 2.** Fluence-to-absorbed dose conversion coefficients ( $D_T/\Phi$ ) for ovaries, uterus, urinary bladder and skin in AP geometry.

in UFH/NCI phantom from 2 to 10 MeV of proton energy and these differences occurred due to the difference in voxel size between ICRP and UFH/NCI phantoms, which in the former is  $1.775 \times 1.775 \times 4.84 \text{ mm}^3$  while in the later is  $3 \times 3 \times 3 \text{ mm}^3$ . In Breast, below 30 MeV, conversion coefficients were much higher in the ICRP reference phantom since in the UFH/NCI there is a layer of adipose tissue around the breasts that reduces proton energy. Although, it was observed high differences in absorbed dose conversion coefficients between the ICRP reference female and the UFH/NCI female phantom, the magnitude of conversion coefficients of both phantoms is the same, especially at energies higher than 100 MeV. The difference observed in conversion coefficients is due to structural differences between the ICRP and the UFH/NCI female phantom.

The calculated fluence-to-absorbed dose conversion coefficients in units of  $\text{pGy cm}^2$ , are given in attached tables B.1–B.6 for the 27 organs of the standing and sitting UFH/NCI female phantom. As presented in tables B.1–B.6, statistical uncertainties for most organs irradiated in antero-posterior (AP), postero-anterior (PA), right lateral (RLAT), left lateral (LLAT), rotational (ROT) and isotropic (ISO) geometry are less than 10% considering  $10^8$  particle histories in each simulation. For smallest and/or deeper organs (such as ovaries, adrenals, thymus, pancreas and kidneys), the statistical uncertainties are beyond 10% since fewer number of particles interacts in these organs. Minor statistical uncertainties were observed in organs that are uniformly distributed in the body, such as skin, RBM, bone surface and muscle for almost all proton energies studied.

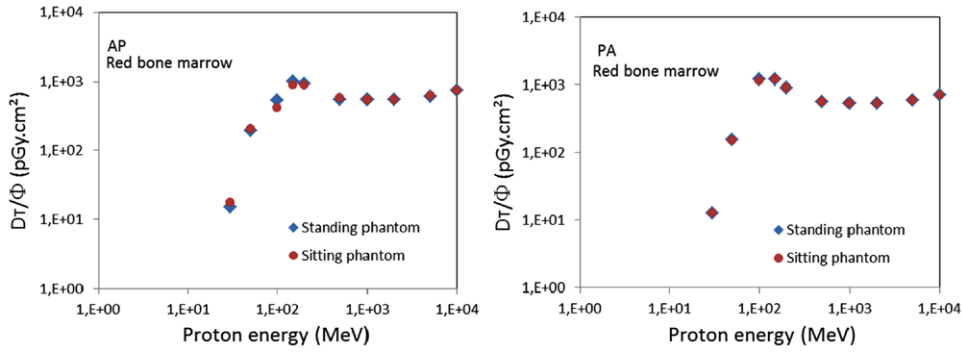


**Figure 3.** Fluence-to-absorbed dose conversion coefficients ( $D_T/\Phi$ ) for red bone marrow in AP and PA geometry.

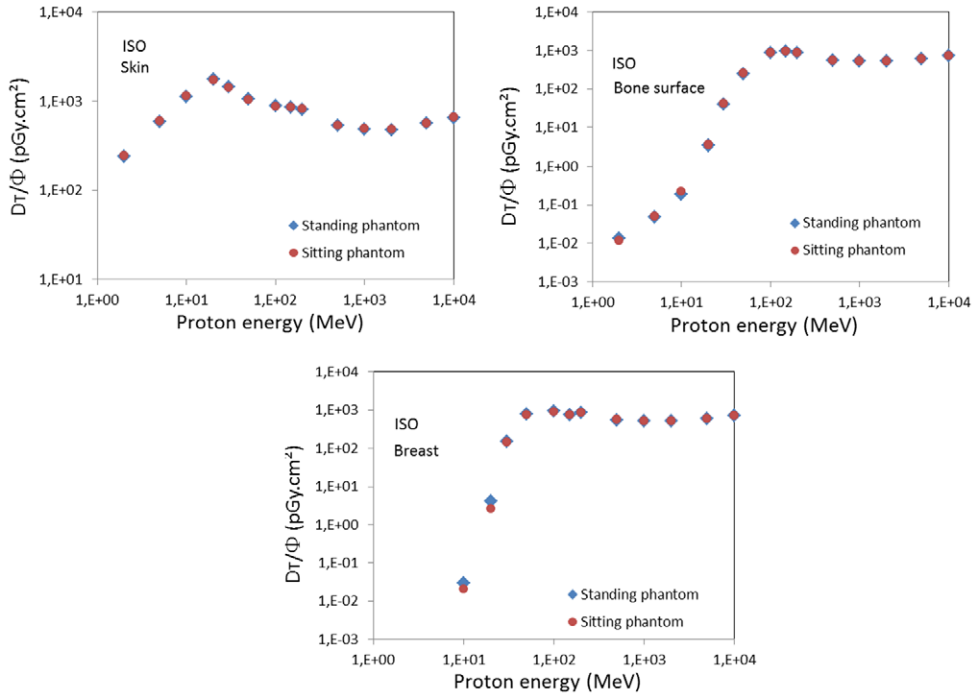


**Figure 4.** Fluence-to-absorbed dose conversion coefficients ( $D_T/\Phi$ ) for skin, bone surface and breast in ISO geometry.

Tables B.1–B.6 also presents the comparison of fluence-to-absorbed dose conversion coefficients of all relevant organs in both postures for AP, PA, RLAT, LLAT, ROT and ISO geometry. Relative differences (RD) between standing and sitting UFH/NCI simulator were calculated using the following equation (1):

$$RD(\%) = \left( \frac{CC(sitting) - CC(standing)}{CC(standing)} \right) \quad (1)$$

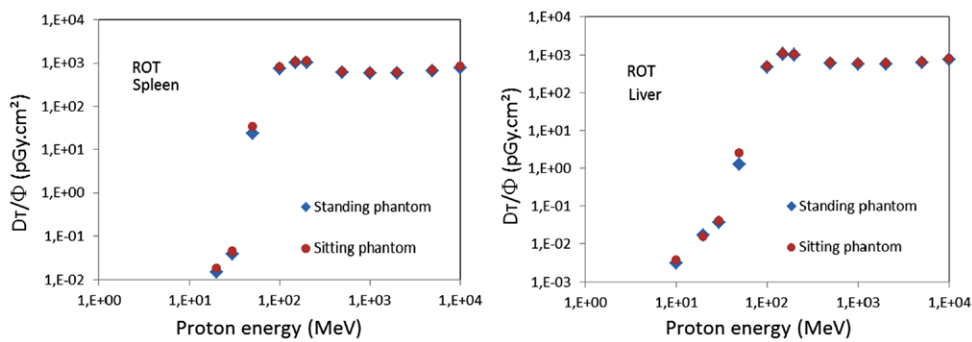


**Figure 5.** Fluence-to-absorbed dose conversion coefficients ( $D_T/\Phi$ ) for spleen and liver in ROT geometry.

As seen in tables B.1–B.6, less than 5% or no relevant differences in conversion coefficients occur for some organs and tissue such as extrathoracic region, oral mucosa, salivary glands and tonsils in all geometry and almost all energies studied. No significant differences between conversion coefficients in standing and sitting postures for these organs occurred because the change in posture did not affect the energy which is deposited.

However in organs located in pelvic and lower abdominal region (ovaries, uterus, bladder, colon and small intestine) differences in conversion coefficients were observed for AP geometry as can be seen in figure 2. In ovaries, uterus and bladder the conversion coefficients until 150 MeV of proton energy are between 25 and 50% higher in the standing phantom and above this energy the conversion coefficients for the sitting phantom are around 10% higher. Anatomical differences caused by changing the posture of the phantom lead an attenuation of incident protons with energies below 150 MeV by the thigh of the phantom in the sitting posture. In colon and small intestine, the phantom thigh, arms and hands located in front of the body also contribute to reducing the energy of incident protons with low energy (below 50 MeV), but the differences in conversion coefficients are around 20%. In skin (figure 2), bone surface and muscle the conversion coefficients of the phantom in standing posture were also higher than in sitting posture. Differences occur because protons have an interaction area with these tissues higher in the standing phantom, so the energy deposited was also higher in this posture. Between 10 and 30 MeV the conversion coefficients for bone surface in the sitting phantom were higher. It occurred because the arms and hands are placed in front of the phantom perpendicular to the beam and therefore protons lose energy in these structures in sitting phantom more than in standing phantom at very low energy, contributing to dose in bone surface.

In PA geometry, however, the thigh of the phantom did not attenuate the incident beam in organs located in pelvic and lower abdominal region, so differences in conversion coefficients was not observed, except for ovaries, uterus and urinary bladder which presented differences between 10 and 30% below 100 MeV of proton energy. Differences in conversion coefficients in skin, muscle and bone surface in PA geometry were similar to the AP geometry, the standing phantom presented conversion coefficients higher than the sitting phantom. As presented in figure 3, in all energies simulated, red bone marrow did not present differences in conversion coefficients because in PA geometry the change in posture did not affect bones that have a higher concentration of red marrow, like sacrum, pelvis and spine. Minor structure differences contribute to conversion coefficients of thyroid in the standing phantom be 47% greater than in the sitting phantom at 100 MeV of protons energy.

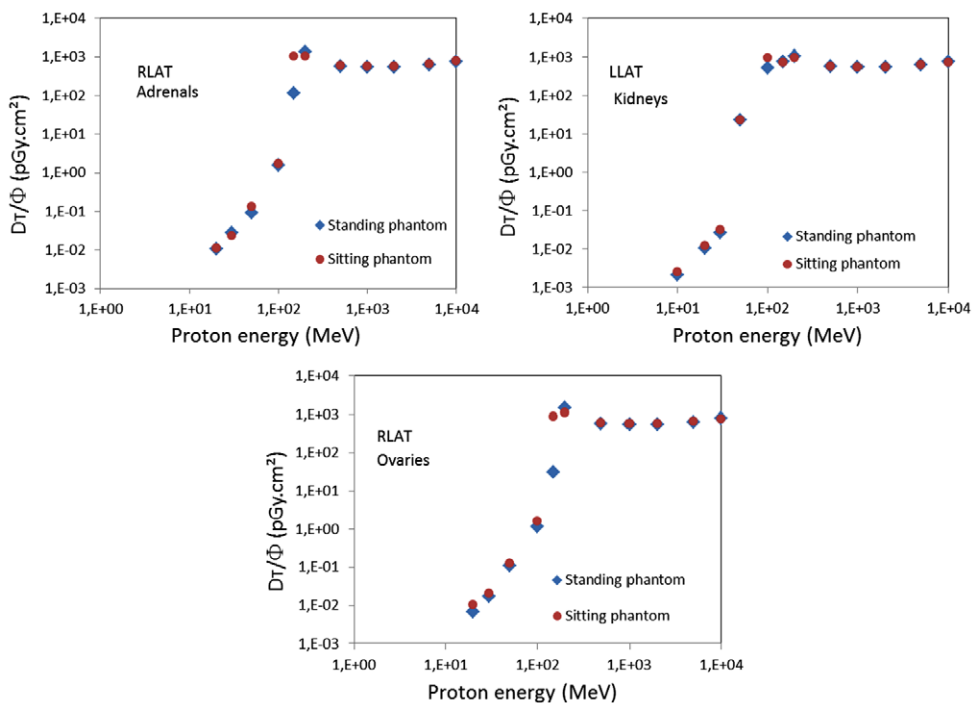


**Figure 6.** Fluence-to-absorbed dose conversion coefficients ( $D_T/\Phi$ ) for adrenals and ovaries in RLAT geometry and kidneys in LLAT geometry.

In isotropic geometry the phantoms are irradiated in all directions with the same probability. This explains there were no significant differences in conversion coefficients in skin and bone surface, since protons can hit these tissues equally in both posture. However, some organ dose conversion coefficients presented significant differences in this irradiation geometry as presented in figure 4. In breast, for example, the conversion coefficient in the standing phantom was higher than in sitting phantom from 20 to 100 MeV, because the thigh of the phantom in the sitting posture attenuates the beam in bottom to head direction. Similarly, in liver, spleen, colon and uterus the phantom thigh leads to differences in conversion coefficients, but in these organs the conversion coefficients in standing phantom were lower because in the standing posture the legs and thigh attenuates the beam in upward direction and the arms attenuates the beam in lateral irradiation, resulting in less dose in these organs in low energy region. Also in ovaries, small intestine and urinary bladder were observed differences in organ dose conversion coefficients, however in the sitting phantom the values were higher until 100 MeV. Differences around 10% in conversion coefficients were observed in other organs and tissues.

In rotational geometry the results of comparison of conversion coefficients in both postures were similar to the isotropic geometry. In liver, spleen (figure 5) and kidneys the arms and hands in the lateral of the body attenuates the beam in the standing phantom while in the sitting posture the arms are in front the phantom, so this structure did not attenuate the beam in these organs. However, some organs and tissues that presented differences in organ dose conversion coefficients in ISO geometry because of the attenuation of the beam by the

**Table 1.** Effective dose per unit fluence ( $\text{pSv}\cdot\text{cm}^2$ ) under AP, PA, RLAT, LLAT, ROT and ISO geometry on UFH/NCI from monoenergetic protons.

AP	Sitting phantom		Standing phantom		
Proton energy (MeV)	$E/\Phi$ ( $\text{pSv}\cdot\text{cm}^2$ )	Relative error	$E/\Phi$ ( $\text{pSv}\cdot\text{cm}^2$ )	Relative error	Relative difference (RD)
2	5.63	0.01%	6.68	0.01%	-15.7%
5	14.05	0.01%	16.67	0.01%	-15.7%
10	28.03	0.01%	33.27	0.01%	-15.8%
20	39.80	0.02%	45.93	0.18%	-13.4%
30	91.57	0.07%	94.07	0.15%	-2.7%
50	736.98	0.07%	737.03	0.11%	0.0%
100	1930.89	0.03%	2038.50	0.04%	-5.3%
150	2315.52	0.04%	2354.52	0.04%	-1.7%
200	1807.87	0.04%	1805.96	0.04%	0.1%
500	1166.69	0.05%	1137.24	0.05%	2.6%
1000	1103.56	0.06%	1078.06	0.07%	2.4%
2000	1099.60	0.08%	1078.92	0.09%	1.9%
5000	1244.36	0.09%	1218.53	0.11%	2.1%
10000	1478.12	0.09%	1449.75	0.12%	2.0%
PA	Sitting phantom		Standing phantom		
Proton energy (MeV)	$E/\Phi$ ( $\text{pSv}\cdot\text{cm}^2$ )	Relative error	$E/\Phi$ ( $\text{pSv}\cdot\text{cm}^2$ )	Relative error	Relative difference (RD)
2	5.64	0.01%	6.69	0.01%	-15.7%
5	14.08	0.01%	16.70	0.01%	-15.7%
10	28.08	0.01%	33.31	0.01%	-15.7%
20	36.15	0.01%	43.45	0.01%	-16.8%
30	31.83	0.02%	38.37	0.02%	-17.1%
50	79.02	0.04%	85.96	0.04%	-8.1%
100	1041.48	0.04%	1069.36	0.05%	-2.6%
150	2657.92	0.05%	2673.21	0.05%	-0.6%
200	1941.82	0.04%	1948.71	0.04%	-0.4%
500	1177.86	0.05%	1184.05	0.05%	-0.5%
1000	1116.53	0.06%	1122.66	0.07%	-0.5%
2000	1116.68	0.07%	1118.76	0.09%	-0.2%
5000	1253.82	0.08%	1255.28	0.10%	-0.1%
10000	1498.64	0.10%	1499.97	0.11%	-0.1%
RLAT	Sitting phantom		Standing phantom		
Proton energy (MeV)	$E/\Phi$ ( $\text{pSv}\cdot\text{cm}^2$ )	Relative error	$E/\Phi$ ( $\text{pSv}\cdot\text{cm}^2$ )	Relative error	Relative difference (RD)
2	4.61	0.02%	3.99	0.01%	15.4%
5	11.50	0.02%	9.96	0.01%	15.4%
10	22.94	0.02%	19.88	0.01%	15.4%
20	32.47	0.04%	29.70	0.07%	9.3%
30	55.06	0.10%	55.08	0.21%	0.0%
50	215.36	0.10%	220.21	0.18%	-2.2%

(Continued)

**Table 1.** (Continued)

100	830.43	0.08%	1052.08	0.07%	-21.1%
150	1671.55	0.07%	1657.79	0.04%	0.8%
200	2020.41	0.07%	2083.33	0.05%	-3.0%
500	1154.42	0.07%	1145.19	0.05%	0.8%
1000	1097.74	0.08%	1086.54	0.06%	1.0%
2000	1102.17	0.10%	1090.47	0.07%	1.1%
5000	1258.36	0.10%	1248.29	0.08%	0.8%
10000	1505.91	0.11%	1493.28	0.09%	0.8%
<hr/>					
LLAT	Sitting phantom		Standing phantom		
Proton energy (MeV)	$E/\Phi$ ( $\text{pSv}\cdot\text{cm}^2$ )	Relative error	$E/\Phi$ ( $\text{pSv}\cdot\text{cm}^2$ )	Relative error	Relative difference (RD)
2	4.61	0.02%	3.99	0.01%	15.4%
5	11.50	0.02%	9.96	0.01%	15.4%
10	22.94	0.02%	19.87	0.01%	15.4%
20	32.85	0.04%	29.39	0.09%	11.7%
30	56.42	0.10%	53.92	0.22%	4.6%
50	228.29	0.10%	214.28	0.19%	6.5%
100	1003.76	0.08%	818.21	0.07%	22.7%
150	1866.91	0.07%	1512.14	0.04%	23.5%
200	2031.56	0.06%	2120.64	0.05%	-4.2%
500	1152.96	0.07%	1146.85	0.05%	0.5%
1000	1094.24	0.08%	1090.54	0.06%	0.3%
2000	1096.98	0.10%	1094.02	0.07%	0.3%
5000	1249.95	0.10%	1257.07	0.08%	-0.6%
10000	1493.46	0.11%	1504.42	0.09%	-0.7%
<hr/>					
ROT	Sitting phantom		Standing phantom		
Proton energy (MeV)	$E/\Phi$ ( $\text{pSv}\cdot\text{cm}^2$ )	Relative error	$E/\Phi$ ( $\text{pSv}\cdot\text{cm}^2$ )	Relative error	Relative difference (RD)
2	6.09	0.03%	6.23	0.02%	-2.2%
5	15.07	0.03%	15.40	0.03%	-2.2%
10	29.27	0.03%	29.84	0.06%	-1.9%
20	44.09	0.05%	44.62	0.30%	-1.2%
30	75.89	0.15%	76.48	0.42%	-0.8%
50	342.47	0.19%	344.59	0.31%	-0.6%
100	1345.91	0.10%	1373.67	0.11%	-2.0%
150	2259.85	0.11%	2213.63	0.10%	2.1%
200	2100.67	0.09%	2001.42	0.09%	5.0%
500	1243.43	0.11%	1187.04	0.11%	4.8%
1000	1177.59	0.14%	1123.13	0.14%	4.8%
2000	1179.77	0.17%	1126.02	0.17%	4.8%
5000	1331.60	0.18%	1275.28	0.20%	4.4%
10000	1591.02	0.20%	1521.78	0.21%	4.5%

(Continued)

**Table 1.** (*Continued*)

ISO	Sitting phantom		Standing phantom		
	Proton energy (MeV)	$E/\Phi$ ( $\text{pSv}\cdot\text{cm}^2$ )	Relative error	$E/\Phi$ ( $\text{pSv}\cdot\text{cm}^2$ )	Relative error
2	4.87	0.02%	4.79	0.02%	1.6%
5	12.00	0.02%	11.83	0.03%	1.5%
10	23.06	0.02%	22.83	0.05%	1.0%
20	37.07	0.04%	37.84	0.21%	-2.0%
30	72.48	0.10%	75.86	0.34%	-4.5%
50	278.73	0.13%	289.50	0.26%	-3.7%
100	983.70	0.08%	1032.77	0.11%	-4.8%
150	1761.77	0.08%	1773.59	0.08%	-0.7%
200	1848.62	0.06%	1849.09	0.08%	0.0%
500	1159.04	0.07%	1154.32	0.08%	0.4%
1000	1100.59	0.09%	1094.25	0.10%	0.6%
2000	1105.76	0.11%	1097.23	0.13%	0.8%
5000	1269.48	0.14%	1262.52	0.14%	0.6%
10000	1519.14	0.14%	1505.09	0.15%	0.9%

phantom thigh in bottom to head direction, such as breast, in ROT geometry these differences in conversion coefficients were not observed.

In RLAT and LLAT geometry the thigh of the phantom did not contribute directly to differences in conversion coefficients in organs located in pelvic and lower abdominal region, but the absorbed-dose conversion coefficients are affected by the arms and hands of the phantom that in the standing posture are in the lateral region of the body and in the sitting posture are in front the phantom. In adrenals, kidneys and ovaries (see figure 6), for example, the absorbed-dose conversion coefficients were higher for the sitting posture until 150 MeV of protons energy as can be seen in tables B.3–B.4, since the phantom arms attenuate the proton beam, resulting in lower dose in these organs. However, at 200 MeV of protons energy, the organ-dose conversion coefficient was higher in the standing posture. The differences observed in skin-dose conversion coefficients are due to the different areas of interaction between the protons and the tissue in both postures, so the conversion coefficient were higher in the sitting phantom because in this posture the area of interaction is larger, since the arms and hands are in front the phantom and contribute to the dose in skin. Some organs, such as brain, breast, extrathoracic region, oral mucosa, salivary glands, thymus, thyroid and tonsils, presented differences less than 10% in conversion coefficients because the change in posture did not affect the dose deposition.

Table 1 lists the results for fluence-to-effective dose conversion coefficients in both postures for AP, PA, LLAT, RLAT, ROT and ISO geometry, in units of  $\text{pSv cm}^2$ , and the statistical error percentages propagated from organ absorbed doses. Fluence-to-effective dose conversion coefficients were calculated from organ-dose conversion coefficients calculated only for the female phantom. The reason for doing this methodology was to examine the influence in conversion coefficients due to the change in the phantom posture, but as recommended in ICRP 2010, the effective dose must be calculated using the Sex-average equivalent doses obtained from the average of equivalent dose of male and female phantoms. In AP geometry, 15% differences in fluence-to-effective dose conversion coefficients were observed between 2 to 20 MeV. This occur because the major contribution to effective

dose at low energies is the skin dose and the fluence-to-skin dose in standing phantom is higher than in sitting phantom between 2 to 20 MeV. As the proton energy increase there's no differences in conversion coefficients in all geometry. Results from comparison of fluence-to-effective dose conversion coefficients in PA geometry are very similar to the AP geometry. In isotropic and rotational irradiation geometry less than 5% differences between conversion coefficients of both postures were observed in all energy simulated. In RLAT and LLAT geometries the fluence-to-effective dose conversion coefficients were around 15% between 2 and 20 MeV and at 100 and 150 MeV, but in the remaining energies there are no significant differences. In this case the conversion coefficients in the sitting phantom were higher because the skin dose conversion coefficients, which between 2 and 20 MeV of proton energy contribute more to the effective dose than other tissues, were higher in the sitting phantom.

#### 4. Conclusions

Comprehensive sets of organ and effective dose conversion coefficients for external proton beams in idealized irradiation geometries were calculated from two UFH/NCI adult female phantoms in standing and sitting postures. The values depend significantly on the morphology and the irradiation geometry, especially at lower energies (below 150 MeV). Change the posture lead to differences in energy deposition in organ and tissue. In antero-posterior geometry the major cause to differences in conversion coefficients is the position of the thigh of the computational phantom, for example, ovaries, uterus and urinary bladder presented conversion coefficients 50% higher in the standing phantom at 30 MeV. In lateral geometries the main contributor to differences in organ-dose conversion coefficients are the position of arms and hands, for example, in organs located in abdominal region such as adrenals, kidneys and pancreas the sitting phantom presented conversion coefficients more than 50% higher at 100 and 150 MeV. In rotational and isotropic geometry the thigh, arms and hands contribute to differences in organ-dose, but the phantoms are irradiated in many directions, so the contribution to differences in conversion coefficients is smaller than in AP, PA, RLAT and LLAT geometries. Since the absence of a set of conversion coefficients for proton source using sitting phantom in literature, this study contributed to filling this lack in addition to providing results more consistent for real exposure scenarios.

**Table A.1.** Absorbed dose per unit fluence ( $\text{pGy cm}^2$ ) under AP geometry from monoenergetic protons for ICRP reference female phantom and UFH/NCI female phantom in standing posture.

AP	Energy (MeV)	$D_T/\Phi$ ( $\text{pGy cm}^2$ )	$D_T/\Phi$ ( $\text{pGv cm}^2$ )	Relative difference (%)	Energy (MeV)	$D_T/\Phi$ ( $\text{pGy cm}^2$ )	$D_T/\Phi$ ( $\text{pGv cm}^2$ )	Relative difference (%)
		(reference female phantom)	(UF/NCI female phantom)			(reference female phantom)	(UF/NCI female phantom)	
Skin	2	604	334	-45%	2			
	5	1510	834	-45%	5			
	10	3020	1663	-45%	10	0.007	0.005	-19%
	20	2320	2182	-6%	20	0.05	3.4	6267%
	30	1720	1721	0%	30	0.6	15.2	2424%
	50	1260	1288	2%	50	236	196	-17%
	100	1030	1061	3%	100	795	540	-32%
	150	1020	953	-7%	150	1370	1013	-26%
	200	853	877	3%	200	924	939	2%
	500	537	530	-1%	500	589	557	-5%
	1000	488	487	0%	1000	571	558	-2%
	2000	486	478	-2%	2000	591	554	-6%
	5000	517	552	7%	5000	641	616	-4%
	10000	590	637	8%	10000	773	740	-4%
Breast	2				2			
	5				5			
	10	1.25	0.01	-99%	10			
	20	1200	0.49	-100%	20	0.04	0.02	-60%
	30	2140	214	-90%	30	0.1	0.04	-59%
	50	2650	2054	-22%	50	0.5	0.2	-47%
	100	1360	1444	6%	100	1330	2.5	-100%
	150	985	994	1%	150	1280	1404	10%
	200	807	812	1%	200	928	953	3%
	500	528	525	-1%	500	616	603	-2%
	1000	471	481	2%	1000	595	571	-4%
	2000	465	475	2%	2000	625	573	-8%
	5000	486	560	15%	5000	659	631	-4%
	10000	523	646	23%	10000	807	762	-6%

**Table A.2.** Absorbed dose per unit fluence ( $\text{pGy cm}^2$ ) under PA geometry from monoenergetic protons for ICRP reference female phantom and UFH/NCI female phantom in standing posture.

PA	Energy (MeV)	$D_T/\Phi$ ( $\text{pGy cm}^2$ )	$D_T/\Phi$ ( $\text{pGv cm}^2$ )	Relative difference (%)	Energy (MeV)	$D_T/\Phi$ ( $\text{pGy cm}^2$ )	$D_T/\Phi$ ( $\text{pGv cm}^2$ )	Relative difference (%)
		(reference female phantom)	(UF/NCI female phantom)			(reference female phantom)	(UF/NCI female phantom)	
Skin	2	605	334	-45%	2			
	5	1510	835	-45%	5			
	10	3020	1665	-45%	10	0.005	0.005	13%
	20	2150	2138	-1%	20	0.03	0.6	1575%
	30	1590	1655	4%	30	0.1	12.7	10096%
	50	1200	1239	3%	50	104	154	48%
	100	1040	1057	2%	100	1200	1186	-1%
	150	1030	950	-8%	150	1260	1213	-4%
	200	854	881	3%	200	904	906	0%
	500	542	530	-2%	500	597	573	-4%
	1000	500	487	-3%	1000	590	544	-8%
	2000	500	477	-5%	2000	611	541	-11%
	5000	559	552	-1%	5000	676	598	-11%
	10000	634	638	1%	10000	801	719	-10%
Breast	2				2			
	5				5			
	10	0.0011	0.0018	66%	10	0.005	0.004	-13%
	20	0.014	0.007	-49%	20	0.03	0.02	-41%
	30	0.036	0.017	-53%	30	0.1	0.04	-42%
	50	0.20	0.11	-48%	50	0.4	0.2	-41%
	100	1.99	1.4	-30%	100	285	2.3	-99%
	150	1650	960	-42%	150	1380	1617	17%
	200	1010	1146	13%	200	954	972	2%
	500	646	616	-5%	500	625	598	-4%
	1000	620	581	-6%	1000	618	570	-8%
	2000	630	568	-10%	2000	656	570	-13%
	5000	722	649	-10%	5000	734	637	-13%
	10000	866	764	-12%	10000	874	763	-13%

**Table A.3.** Absorbed dose per unit fluence ( $\text{pGy cm}^2$ ) under RLAT geometry from monoenergetic protons for ICRP reference female phantom and UFH/NCI female phantom in standing posture.

RLAT	Energy (MeV)	$D_T/\Phi$ ( $\text{pGy cm}^2$ )	$D_T/\Phi$ ( $\text{pGv cm}^2$ )	Relative difference (%)	Energy (MeV)	$D_T/\Phi$ ( $\text{pGy cm}^2$ )	$D_T/\Phi$ ( $\text{pGv cm}^2$ )	Relative difference (%)
		(reference female phantom)	(UF/NCI female phantom)			(reference female phantom)	(UF/NCI female phantom)	
Skin	2	307	200	-35%	2			
	5	768	498	-35%	5			
	10	1530	993	-35%	10	0.001	0.003	223%
	20	1190	1321	11%	20	0.02	0.4	2030%
	30	941	1070	14%	30	0.1	9.3	8481%
	50	763	835	9%	50	143	93.3	-35%
	100	895	856	-4%	100	322	379	18%
	150	891	841	-6%	150	775	783	1%
	200	781	770	-1%	200	1010	970	-4%
	500	540	523	-3%	500	597	569	-5%
	1000	500	481	-4%	1000	594	545	-8%
	2000	504	475	-6%	2000	622	545	-12%
	5000	557	559	0%	5000	695	617	-11%
	10 000	643	649	1%	10 000	832	745	-10%
Breast	2				2			
	5				5			
	10	0.017	0.00	-82%	10			
	20	202	0.19	-100%	20	0.007	0.007	5%
	30	429	77.6	-82%	30	0.023	0.018	-23%
	50	762	536	-30%	50	0.10	0.11	17%
	100	930	850	-9%	100	0.96	1.3	39%
	150	984	923	-6%	150	84.7	117	38%
	200	968	978	1%	200	1280	1352	6%
	500	575	554	-4%	500	618	585	-5%
	1000	556	513	-8%	1000	653	563	-14%
	2000	563	509	-10%	2000	659	565	-14%
	5000	591	590	0%	5000	783	644	-18%
	10 000	698	691	-1%	10 000	936	774	-17%

**Table A.4.** Absorbed dose per unit fluence ( $\text{pGy cm}^2$ ) under ISO geometry from monoenergetic protons for ICRP reference female phantom and UFH/NCI female phantom in standing posture.

ISO	Energy (MeV)	$D_T/\Phi$ ( $\text{pGy cm}^2$ )	$D_T/\Phi$ ( $\text{pGv cm}^2$ )	Relative difference (%)	Energy (MeV)	$D_T/\Phi$ ( $\text{pGy cm}^2$ )	$D_T/\Phi$ ( $\text{pGv cm}^2$ )	Relative difference (%)
		(reference female phantom)	(UF/NCI female phantom)			(reference female phantom)	(UF/NCI female phantom)	
Skin	2	385	239	-38%	2			
	5	944	589	-38%	5			
	10	1780	1132	-36%	10	0.083	0.058	-30%
	20	1870	1765	-6%	20	0.34	1.12	232%
	30	1420	1451	2%	30	7.4	15.0	101%
	50	1030	1063	3%	50	109	116	7%
	100	867	892	3%	100	497	492	-1%
	150	880	859	-2%	150	966	877	-9%
	200	818	809	-1%	200	917	916	0%
	500	538	529	-2%	500	589	576	-2%
	1000	492	486	-1%	1000	578	548	-5%
	2000	498	479	-4%	2000	617	548	-11%
	5000	567	561	-1%	5000	712	622	-13%
	10000	672	651	-3%	10000	893	750	-16%
Breast	2				2			
	5				5			
	10	40.5	0.03	-100%	10			
	20	311	4.1	-99%	20	0.02	0.01	-34%
	30	629	154	-76%	30	0.04	0.02	-40%
	50	996	785	-21%	50	0.17	0.16	-6%
	100	858	960	12%	100	131	22.8	-83%
	150	831	754	-9%	150	848	939	11%
	200	913	871	-5%	200	1010	1000	-1%
	500	574	556	-3%	500	598	599	0%
	1000	538	518	-4%	1000	598	570	-5%
	2000	550	514	-7%	2000	661	577	-13%
	5000	632	601	-5%	5000	785	662	-16%
	10000	758	705	-7%	10000	1020	791	-22%

**Table B.1.** Absorbed dose per unit fluence (pGy cm<sup>2</sup>) under AP geometry from monoenergetic protons for UFH/NCl in standing and sitting posture.

AP		Sitting phantom			Standing phantom			Sitting phantom			Standing phantom		
Energy (MeV)	$D_{T/\Phi}$ (pGy cm <sup>2</sup> )	Relative error	$D_{T/\Phi}$ (pGy cm <sup>2</sup> )	Relative difference (RD)	$D_{T/\Phi}$ (pGy cm <sup>2</sup> )	Relative error	$D_{T/\Phi}$ (pGy cm <sup>2</sup> )	Relative difference (RD)	$D_{T/\Phi}$ (pGy cm <sup>2</sup> )	Relative error	$D_{T/\Phi}$ (pGy cm <sup>2</sup> )	Relative error	
5	5												
10	0.0106	9.5%	0.0117	11.0%	-10.1%	0.00259	5.3%	0.00260	5.9%	-0.6%	0.0105	3.6%	
20	0.025	7.4%	0.023	7.9%	7.8%	0.0126	2.5%	0.0128	2.8%	-1.7%	0.49	1.8%	
30	0.05	11.4%	0.15	9.1%	8.2%	0.0339	1.8%	0.0337	2.3%	0.5%	214.36	0.1%	
50	0.16	6.0%	1.69	6.9%	5.9%	64.56	0.2%	64.36	0.2%	0.3%	2056.17	0.1%	
100	0.80	6.0%	1.69	6.9%	6.9%	767.70	0.1%	767.65	0.1%	0.0%	1445.58	0.1%	
150	88.63	1.1%	88.34	1.2%	0.3%	1387.21	0.1%	1387.34	0.1%	0.0%	994.70	0.1%	
200	1083.29	0.3%	1077.82	0.3%	0.5%	925.90	0.1%	925.99	0.1%	0.0%	813.62	0.1%	
500	613.98	0.4%	604.68	0.4%	1.5%	561.04	0.1%	561.18	0.1%	0.0%	527.89	0.1%	
1000	592.94	0.5%	590.82	0.6%	0.4%	525.06	0.1%	525.23	0.1%	0.0%	485.71	0.1%	
2000	596.59	0.6%	589.47	0.7%	1.2%	526.91	0.1%	526.50	0.1%	0.1%	480.64	0.1%	
5000	656.07	0.6%	657.23	0.8%	-0.2%	600.19	0.1%	600.44	0.1%	0.0%	563.54	0.2%	
10000	791.91	0.8%	786.87	0.7%	0.6%	715.38	0.1%	715.92	0.2%	-0.1%	650.79	0.2%	
AP		Sitting phantom			Standing phantom			Sitting phantom			Standing phantom		
Energy (MeV)	$D_{T/\Phi}$ (pGy cm <sup>2</sup> )	Relative error	$D_{T/\Phi}$ (pGy cm <sup>2</sup> )	Relative difference (RD)	$D_{T/\Phi}$ (pGy cm <sup>2</sup> )	Relative error	$D_{T/\Phi}$ (pGy cm <sup>2</sup> )	Relative difference (RD)	$D_{T/\Phi}$ (pGy cm <sup>2</sup> )	Relative error	$D_{T/\Phi}$ (pGy cm <sup>2</sup> )	Relative error	
5	5												
10	0.0040	4.2%	0.0048	4.3%	-16%	0.016	5.4%	0.015	6.3%	2.9%	0.02	6.8%	0.01
20	0.019	2.1%	0.024	2.1%	-23%	0.035	3.9%	0.035	4.1%	0.3%	0.04	5.0%	0.04
30	0.05	1.5%	0.06	1.6%	-17%	0.21	5.3%	0.20	4.8%	8.2%	0.23	11.0%	0.24
50	0.25	1.7%	0.28	1.8%	-11%	459.06	0.3%	465.09	0.4%	-1.3%	2.40	5.0%	2.21
100	1216.17	0.1%	1255.07	0.1%	-3%	1872.54	0.2%	1873.66	0.2%	-0.1%	1456.03	0.2%	1452.82
150	1244.23	0.1%	1252.03	0.1%	-1%	968.75	0.2%	966.93	0.2%	0.2%	959.98	0.3%	959.98
200	915.73	0.1%	902.36	0.1%	1%	597.53	0.2%	595.49	0.2%	0.3%	610.71	0.3%	603.94
500	604.98	0.1%	578.06	0.1%	5%	567.09	0.3%	567.02	0.3%	0.0%	579.11	0.5%	572.95
1000	573.46	0.1%	546.00	0.1%	5%	567.44	0.4%	566.37	0.4%	0.2%	573.69	0.6%	568.27
2000	571.12	0.1%	548.15	0.2%	4%	637.09	0.4%	635.95	0.5%	0.2%	641.90	0.7%	642.06
5000	639.91	0.1%	615.64	0.2%	4%	762.09	0.5%	763.36	0.6%	-0.2%	769.96	0.8%	770.18
10000	761.28	0.2%	734.86	0.2%									

(Continued)

**Table B.1.** (*Continued*)

AP		Sitting phantom			Standing phantom			Sitting phantom			Standing phantom						
Energy (MeV)	$D_{\gamma}/\phi$ (pGy cm <sup>2</sup> )	Relative error	$D_{\gamma}/\phi$ (pGy cm <sup>2</sup> )	Relative difference (RD)	$D_{\gamma}/\phi$ (pGy cm <sup>2</sup> )	Relative error	$D_{\gamma}/\phi$ (pGy cm <sup>2</sup> )	Relative difference (RD)	$D_{\gamma}/\phi$ (pGy cm <sup>2</sup> )	Relative error	$D_{\gamma}/\phi$ (pGy cm <sup>2</sup> )	Relative error					
Heart	2	5	0.00	5.1%	0.005	5.8%	6%	0.002	8.1%	0.003	8.3%	-26%	0.00426	4.0%	0.00429	4.4%	-1%
	10	0.02	2.5%	0.02	2.8%	1%	0.009	3.9%	0.012	4.1%	-21%	0.019	1.9%	0.020	2.1%	-3%	
	20	0.05	1.8%	0.05	2.5%	-2%	0.021	3.1%	0.025	3.2%	-15%	0.045	1.4%	0.046	1.6%	-1%	
	50	0.26	1.8%	0.26	2.0%	1%	0.13	3.0%	0.13	2.9%	-2%	0.24	1.1%	0.23	1.3%	1%	
	100	1058.34	0.1%	1059.92	0.1%	0%	1.51	1.7%	1.58	1.9%	-4%	830.74	0.1%	832.56	0.1%	-0.2%	
	150	1316.50	0.1%	1317.15	0.1%	0%	326.95	0.2%	326.81	0.2%	0%	1305.66	0.1%	1308.05	0.1%	-0.2%	
	200	912.78	0.1%	913.38	0.1%	0%	1102.25	0.1%	1101.36	0.1%	0%	940.98	0.1%	942.16	0.1%	-0.1%	
	500	580.71	0.1%	579.46	0.1%	0%	609.91	0.1%	598.44	0.1%	0%	590.59	0.1%	585.84	0.1%	1%	
	1000	549.60	0.1%	547.63	0.2%	0%	591.61	0.1%	580.32	0.2%	0%	560.63	0.1%	555.63	0.1%	1%	
	2000	550.25	0.2%	547.52	0.2%	0%	586.48	0.2%	578.07	0.2%	0%	561.14	0.1%	556.60	0.1%	1%	
Lungs	5000	615.80	0.2%	614.33	0.2%	0%	659.69	0.2%	654.72	0.2%	0%	627.39	0.1%	624.51	0.1%	0.5%	
	10 000	796.15	0.2%	793.52	0.2%	0%	790.77	0.2%	786.39	0.2%	0%	749.88	0.1%	747.74	0.1%	0.3%	
AP		Sitting phantom			Standing phantom			Sitting phantom			Standing phantom						
Energy (MeV)	$D_{\gamma}/\phi$ (pGy cm <sup>2</sup> )	Relative error	$D_{\gamma}/\phi$ (pGy cm <sup>2</sup> )	Relative difference (RD)	$D_{\gamma}/\phi$ (pGy cm <sup>2</sup> )	Relative error	$D_{\gamma}/\phi$ (pGy cm <sup>2</sup> )	Relative difference (RD)	$D_{\gamma}/\phi$ (pGy cm <sup>2</sup> )	Relative error	$D_{\gamma}/\phi$ (pGy cm <sup>2</sup> )	Relative error					
Extrahepatic region	10	0.0041	3.0%	0.0044	3.3%	-6%	35.51	1.0%	35.63	1.1%	-0.3%	0.023	5.0%	0.026	5.5%	-12%	
	20	0.018	1.4%	0.019	1.7%	-5%	123.29	0.7%	124.55	0.8%	-1%	0.35	7.2%	0.38	7.8%	-8%	
	30	0.045	1.1%	0.046	1.3%	-2%	1073.81	0.3%	1075.57	0.3%	-0.2%	3.64	2.8%	3.78	3.1%	-4%	
	50	1.174	0.9%	1.171	1.0%	0.3%	1475.68	0.2%	1481.39	0.2%	-0.4%	1722.13	0.2%	1717.11	0.2%	0.3%	
	100	1443.99	0.1%	1444.28	0.1%	0.0%	1128.38	0.1%	1011.36	0.2%	0.2%	1147.26	0.2%	1140.50	0.2%	1%	
	150	1129.41	0.1%	1128.39	0.1%	0.1%	895.27	0.1%	822.11	0.2%	0.2%	871.01	0.2%	869.70	0.2%	0.2%	
	200	896.39	0.1%	895.27	0.1%	0.1%	570.65	0.1%	540.97	0.3%	0.3%	547.85	0.2%	545.01	0.3%	1%	
	500	573.04	0.1%	572.22	0.1%	0.4%	507.58	0.4%	511.90	0.4%	-1%	512.83	0.3%	510.99	0.4%	0.4%	
	1000	539.40	0.1%	535.46	0.1%	1%	504.62	0.5%	507.01	0.5%	-0.5%	514.03	0.4%	513.00	0.4%	0.2%	
	2000	543.73	0.1%	542.31	0.1%	0.3%	578.42	0.5%	578.14	0.6%	0.0%	589.23	0.4%	587.37	0.5%	0.3%	
Oral mucosa	5000	616.68	0.1%	613.31	0.1%	1%	685.57	0.6%	676.27	0.6%	1%	701.50	0.5%	697.44	0.5%	1%	
	10 000	735.94	0.1%	732.22	0.1%	1%											

(Continued)

**Table B.1.** (*Continued*)

AP	Sitting phantom			Standing phantom			Sitting phantom			Standing phantom								
	Energy (MeV)	$D_{\gamma}/\phi$ (pGy cm <sup>2</sup> )	Relative error	$D_{\gamma}/\phi$ (pGy cm <sup>2</sup> )	Relative difference (RD)	$D_{\gamma}/\phi$ (pGy cm <sup>2</sup> )	Relative error	$D_{\gamma}/\phi$ (pGy cm <sup>2</sup> )	Relative difference (RD)	$D_{\gamma}/\phi$ (pGy cm <sup>2</sup> )	Relative error	$D_{\gamma}/\phi$ (pGy cm <sup>2</sup> )	Relative error					
2	5	10	0.01	10.4%	0.02	9.6%	-35%	0.013	4.6%	0.015	5.2%	-14%	0.30	7.0%	0.31	7.7%	-1%	
	20	0.03	8.6%	0.05	6.5%	-50%	0.031	3.5%	0.035	3.7%	-9%	1.57	3.7%	1.62	4.2%	-3%		
Ovaries	50	0.17	12.7%	0.23	5.2%	-24%	0.18	4.0%	0.19	4.4%	-7%	79.91	0.7%	80.34	0.7%	-1%		
Pancreas	100	2.41	5.8%	3.38	5.0%	-29%	1.99	2.1%	1.95	2.3%	2%	1454.47	0.2%	1465.13	0.2%	-1%		
	150	1272.11	0.3%	1235.52	0.3%	2%	2146.10	0.1%	2144.82	0.1%	0.1%	1149.54	0.2%	1145.55	0.2%	0.3%		
	200	947.03	0.3%	924.87	0.4%	2%	1004.37	0.1%	1002.45	0.1%	0.2%	870.72	0.2%	868.36	0.2%	0.3%		
	500	642.59	0.4%	594.70	0.5%	8%	611.43	0.2%	603.38	0.2%	1%	549.56	0.2%	546.71	0.2%	1%		
	1000	613.59	0.5%	559.08	0.6%	10%	583.24	0.2%	573.96	0.2%	2%	511.68	0.3%	509.71	0.3%	0.4%		
	2000	601.91	0.7%	567.06	0.8%	6%	583.07	0.2%	581.26	0.3%	0.3%	512.57	0.3%	509.63	0.4%	1%		
	5000	684.07	0.8%	637.32	0.9%	7%	650.53	0.3%	647.35	0.3%	0.5%	584.92	0.3%	581.72	0.4%	1%		
	10000	809.22	0.8%	755.79	0.9%	7%	778.82	0.3%	779.67	0.3%	-0.1%	688.68	0.4%	688.68	0.5%	0.0%		
AP	Sitting phantom			Standing phantom			Sitting phantom			Standing phantom			Sitting phantom					
	Energy (MeV)	$D_{\gamma}/\phi$ (pGy cm <sup>2</sup> )	Relative error	$D_{\gamma}/\phi$ (pGy cm <sup>2</sup> )	Relative difference (RD)	$D_{\gamma}/\phi$ (pGy cm <sup>2</sup> )	Relative error	$D_{\gamma}/\phi$ (pGy cm <sup>2</sup> )	Relative difference (RD)	$D_{\gamma}/\phi$ (pGy cm <sup>2</sup> )	Relative error							
2	5	10	0.004	3.8%	0.005	4.1%	-21%	702.41	0.0%	833.72	0.0%	-16%	334.04	0.0%	334.04	0.0%	-16%	
	20	0.016	2.0%	0.021	2.0%	-24%	1400.56	0.0%	1662.70	0.0%	-16%	0.01	5.0%	0.02	5.0%	-24%		
	30	0.04	1.4%	0.05	1.5%	-20%	1873.61	0.0%	2182.44	0.0%	-14%	0.034	3.8%	0.034	3.4%	0.0%		
	50	0.23	1.4%	0.25	1.5%	-9%	1569.44	0.0%	1720.57	0.0%	-9%	0.17	3.5%	0.18	4.3%	-1%		
	100	974.47	0.1%	985.47	0.1%	-1%	1031.61	0.0%	1060.75	0.0%	-3%	1.145	1.1%	11.44	1.3%	1.3%		
	150	1333.17	0.1%	1325.42	0.1%	1%	913.36	0.0%	952.76	0.0%	-4%	1482.50	0.2%	1484.02	0.2%	-0.1%		
	200	935.61	0.1%	925.30	0.1%	1%	864.06	0.0%	877.50	0.0%	-2%	989.12	0.2%	989.60	0.2%	0.0%		
	500	611.69	0.1%	587.12	0.1%	4%	533.73	0.0%	529.55	0.0%	1%	597.40	0.2%	589.11	0.2%	1%		
	1000	580.18	0.1%	553.90	0.1%	5%	491.16	0.0%	486.63	0.0%	1%	568.01	0.2%	561.15	0.3%	1%		
	2000	577.34	0.1%	555.93	0.1%	4%	482.14	0.0%	477.56	0.0%	1%	567.73	0.3%	562.83	0.3%	1%		
	5000	640.98	0.1%	623.11	0.1%	3%	560.58	0.0%	551.67	0.1%	2%	635.60	0.3%	633.03	0.3%	0.4%		
	10000	764.73	0.1%	744.90	0.2%	3%	647.44	0.1%	637.06	0.1%	2%	761.35	0.3%	757.04	0.4%	1%		
Small intestine	Sitting phantom			Standing phantom			Sitting phantom			Standing phantom			Sitting phantom					
	Energy (MeV)	$D_{\gamma}/\phi$ (pGy cm <sup>2</sup> )	Relative error	$D_{\gamma}/\phi$ (pGy cm <sup>2</sup> )	Relative difference (RD)	$D_{\gamma}/\phi$ (pGy cm <sup>2</sup> )	Relative error	$D_{\gamma}/\phi$ (pGy cm <sup>2</sup> )	Relative difference (RD)	$D_{\gamma}/\phi$ (pGy cm <sup>2</sup> )	Relative error							
2	5	10	0.004	3.8%	0.005	4.1%	-21%	281.44	0.0%	334.04	0.0%	-16%						
	20	0.016	2.0%	0.021	2.0%	-24%	1400.56	0.0%	1662.70	0.0%	-16%							
	30	0.04	1.4%	0.05	1.5%	-20%	1873.61	0.0%	2182.44	0.0%	-14%							
	50	0.23	1.4%	0.25	1.5%	-9%	1569.44	0.0%	1720.57	0.0%	-9%							
	100	974.47	0.1%	985.47	0.1%	-1%	1031.61	0.0%	1060.75	0.0%	-3%							
	150	1333.17	0.1%	1325.42	0.1%	1%	913.36	0.0%	952.76	0.0%	-4%							
	200	935.61	0.1%	925.30	0.1%	1%	864.06	0.0%	877.50	0.0%	-2%							
	500	611.69	0.1%	587.12	0.1%	4%	533.73	0.0%	529.55	0.0%	1%							
	1000	580.18	0.1%	553.90	0.1%	5%	491.16	0.0%	486.63	0.0%	1%							
	2000	577.34	0.1%	555.93	0.1%	4%	482.14	0.0%	477.56	0.0%	1%							
	5000	640.98	0.1%	623.11	0.1%	3%	560.58	0.0%	551.67	0.1%	2%							
	10000	764.73	0.1%	744.90	0.2%	3%	647.44	0.1%	637.06	0.1%	2%							
Spleen	Sitting phantom			Standing phantom			Sitting phantom			Standing phantom			Sitting phantom					
	Energy (MeV)	$D_{\gamma}/\phi$ (pGy cm <sup>2</sup> )	Relative error	$D_{\gamma}/\phi$ (pGy cm <sup>2</sup> )	Relative difference (RD)	$D_{\gamma}/\phi$ (pGy cm <sup>2</sup> )	Relative error	$D_{\gamma}/\phi$ (pGy cm <sup>2</sup> )	Relative difference (RD)	$D_{\gamma}/\phi$ (pGy cm <sup>2</sup> )	Relative error							
2	5	10	0.004	3.8%	0.005	4.1%	-21%	702.41	0.0%	833.72	0.0%	-16%						
	20	0.016	2.0%	0.021	2.0%	-24%	1400.56	0.0%	1662.70	0.0%	-16%							
	30	0.04	1.4%	0.05	1.5%	-20%	1873.61	0.0%	2182.44	0.0%	-14%							
	50	0.23	1.4%	0.25	1.5%	-9%	1569.44	0.0%	1720.57	0.0%	-9%							
	100	974.47	0.1%	985.47	0.1%	-1%	1031.61	0.0%	1060.75	0.0%	-3%							
	150	1333.17	0.1%	1325.42	0.1%	1%	913.36	0.0%	952.76	0.0%	-4%							
	200	935.61	0.1%	925.30	0.1%	1%	864.06	0.0%	877.50	0.0%	-2%							
	500	611.69	0.1%	587.12	0.1%	4%	533.73	0.0%	529.55	0.0%	1%							
	1000	580.18	0.1%	553.90	0.1%	5%	491.16	0.0%	486.63	0.0%	1%							
	2000	577.34	0.1%	555.93	0.1%	4%	482.14	0.0%	477.56	0.0%	1%							
	5000	640.98	0.1%	623.11	0.1%	3%	560.58	0.0%	551.67	0.1%	2%							
	10000	764.73	0.1%	744.90	0.2%	3%	647.44	0.1%	637.06	0.1%	2%							
Spleen	Sitting phantom			Standing phantom			Sitting phantom			Standing phantom			Sitting phantom					
	Energy (MeV)	$D_{\gamma}/\phi$ (pGy cm <sup>2</sup> )	Relative error	$D_{\gamma}/\phi$ (pGy cm <sup>2</sup> )	Relative difference (RD)	$D_{\gamma}/\phi$ (pGy cm <sup>2</sup> )	Relative error	$D_{\gamma}/\phi$ (pGy cm <sup>2</sup> )	Relative difference (RD)	$D_{\gamma}/\phi$ (pGy cm <sup>2</sup> )	Relative error							
2	5	10	0.004	3.8%	0.005	4.1%	-21%	702.41	0.0%	833.72	0.0%	-16%						
	20	0.016	2.0%	0.021	2.0%	-24%	1400.56	0.0%	1662.70	0.0%	-16%							
	30	0.04	1.4%	0.05	1.5%	-20%	1873.61	0.0%	2182.44	0.0%	-14%							
	50	0.23	1.4%	0.25	1.5%	-9%	1569.44	0.0%	1720.57	0.0%	-9%							
	100	974.47	0.1%	985.47	0.1%	-1%	1031.61	0.0%	1060.75	0.0%	-3%							
	150	1333.17	0.1%	1325.42	0.1%	1%	913.36	0.0%	952.76	0.0%	-4%							
	200	935.61	0.1%	925.30	0.1%	1%	864.06	0.0%	877.50	0.0%	-2%							
	500	611.69	0.1%	587.12	0.1%	4%	533.73	0.0%	529.55	0.0%	1%							
	1000	580.18	0.1%	553.90	0.1%	5%	491.16	0.0%	486.63	0.0%	1%							
	2000	577.34	0.1%	555.93	0.1%	4%	482.14	0.0%	477.56	0.0%	1%							
	5000	640.98	0.1%	623.11	0.1%	3%	560.58	0.0%	551.67	0.1%	2%							
</																		

**Table B.1.** (Continued)

AP	Sitting phantom			Standing phantom			Sitting phantom			Standing phantom			Sitting phantom			Standing phantom		
	Energy (MeV)	$D_{\gamma}/\phi$ (pGy cm <sup>2</sup> )	Relative error															
2	5	10	0.0048	6.4%	0.0052	7.0%	-7%	0.023	7.0%	0.025	7.6%	-8%	0.035	5.6%	0.031	7.0%	13%	
Stomach	20	0.021	3.3%	0.023	3.4%	0.025	3.4%	-6%	0.065	11.8%	0.055	5.6%	17%	0.3%	1718.94	0.3%	-1%	
2	5	30	0.048	2.4%	0.050	2.6%	-5%	0.065	6.5%	0.35	6.5%	-6%	1700.04	0.3%	1459.46	0.2%	-1%	
2	5	50	0.26	2.6%	0.25	3.0%	3%	0.33	6.5%	0.35	6.5%	Thyroid	1007.24	0.2%	996.49	0.2%	-1%	
2	5	100	1319.71	0.1%	1319.18	0.1%	0.0%	2211.28	0.2%	2199.42	0.3%	Thymus	824.11	0.3%	817.13	0.3%	-1%	
Tonsil	150	1268.75	0.1%	1265.63	0.1%	0.2%	1102.79	0.2%	1097.10	0.3%	1102.79	0.2%	1007.24	0.3%	1007.24	0.3%	-1%	
2	5	200	913.36	0.1%	910.94	0.1%	0.3%	868.33	0.2%	861.70	0.3%	861.70	0.3%	854.97	0.4%	854.97	0.4%	-1%
2	5	500	589.29	0.1%	583.03	0.2%	1%	567.18	0.3%	563.38	0.4%	567.18	0.3%	545.97	0.5%	545.97	0.5%	-1%
2	5	1000	556.25	0.2%	550.34	0.2%	1%	538.44	0.4%	530.43	0.5%	538.44	0.5%	511.30	0.5%	511.30	0.5%	-1%
2	5	2000	556.34	0.2%	550.02	0.2%	1%	535.20	0.5%	526.97	0.6%	535.20	0.5%	507.45	0.6%	507.45	0.6%	-1%
2	5	5000	621.98	0.2%	616.00	0.3%	1%	596.38	0.6%	594.51	0.7%	596.38	0.3%	576.03	0.7%	576.03	0.8%	-1%
2	5	10000	743.63	0.3%	738.53	0.3%	1%	710.85	0.7%	705.51	0.7%	710.85	0.7%	673.32	0.7%	683.63	1.1%	-2%
AP	Sitting phantom			Standing phantom			Sitting phantom			Standing phantom			Sitting phantom			Standing phantom		
Energy (MeV)	$D_{\gamma}/\phi$ (pGy cm <sup>2</sup> )	Relative error	$D_{\gamma}/\phi$ (pGy cm <sup>2</sup> )	Relative error														
2	5	10	0.002	10.5%	0.006	8.1%	-62%	0.01	7.1%	0.01	7.1%	0.02	5.4%	-49%	0.02	5.4%	-49%	
Tonsil	20	0.01	7.4%	0.03	4.0%	-48%	0.01	7.4%	0.03	4.0%	0.02	5.2%	0.04	3.9%	0.04	3.9%	-54%	
2	5	30	0.03	3.7%	0.06	2.9%	-52%	0.03	3.7%	0.06	4.3%	0.14	5.6%	-42%	0.24	4.4%	-42%	
2	5	50	0.17	6.9%	0.18	6.8%	-7%	0.18	5.1%	0.33	4.3%	0.2%	4.5%	1.77	2.8%	2.46	2.5%	-28%
2	5	100	2.44	11.9%	2.33	14.3%	5%	893.75	0.2%	1633.68	0.2%	1138.81	0.2%	1367.51	0.2%	1403.85	0.2%	-3%
2	5	150	1384.25	0.5%	1400.91	0.6%	-1%	1082.96	0.2%	883.90	0.2%	959.93	0.2%	981.39	0.2%	953.05	0.2%	3%
2	5	200	918.88	0.5%	919.44	0.6%	-0.1%	631.71	0.2%	574.73	0.2%	651.47	0.2%	603.16	0.2%	603.16	0.2%	8%
2	5	500	555.01	0.7%	559.80	0.8%	-1%	606.87	0.2%	543.93	0.3%	627.76	0.2%	571.10	0.3%	571.10	0.3%	10%
2	5	1000	522.46	0.9%	523.41	1.1%	-0.2%	604.38	0.3%	547.63	0.4%	620.00	0.3%	572.68	0.3%	572.68	0.3%	8%
2	5	2000	530.04	1.2%	535.11	1.4%	-1%	604.19	0.3%	685.71	0.3%	611.69	0.5%	703.40	0.3%	631.41	0.4%	11%
2	5	5000	603.61	1.9%	604.19	2.3%	-0.1%	814.36	0.5%	732.08	0.6%	826.83	0.3%	761.53	0.5%	761.53	0.5%	9%

(Continued)

**Table B.1.** (*Continued*)

AP	Sitting phantom		Standing phantom		Sitting phantom		Standing phantom		Sitting phantom		Standing phantom			
	Energy (MeV)	$D_{T\phi}$ (pGy cm <sup>2</sup> )	Relative error											
2	0.00093	2.4%	0.00088	2.8%	5%	7%	3.4%	0.008	3.8%	19%	0.004	3.3%	0.005	3.2%
5	0.015	0.9%	0.014	1.0%	5%	0.010	0.2%	7.24	0.3%	8%	3.83	0.2%	3.43	0.3%
10	0.101	0.5%	0.096	0.5%	0.5%	-11%	7.84	0.2%	31.83	0.2%	17.45	0.1%	15.22	0.2%
20	24.14	0.0%	27.27	0.0%	-12%	36.42	0.1%	200.94	0.1%	-3%	205.92	0.1%	196.48	0.1%
30	77.69	0.0%	88.31	0.0%	-17%	195.16	0.1%	1065.22	0.0%	-10%	421.36	0.0%	540.36	0.0%
50	279.01	0.0%	337.99	0.0%	-30%	959.47	0.0%	1050.58	0.0%	-10%	884.54	0.0%	1013.00	0.0%
100	745.12	0.0%	1057.79	0.0%	-21%	944.05	0.0%	831.42	0.0%	-5%	896.00	0.0%	939.37	0.0%
150	912.54	0.0%	1148.22	0.0%	-6%	911.61	0.0%	552.13	0.0%	-5%	536.85	0.0%	578.17	0.0%
200	857.63	0.0%	566.01	0.0%	-1%	523.33	0.0%	530.41	0.0%	-1%	554.65	0.0%	557.76	0.1%
500	559.81	0.0%	532.64	0.0%	-0.3%	520.76	0.1%	525.41	0.1%	-1%	552.45	0.1%	553.72	0.1%
1000	528.06	0.0%	531.96	0.0%	1%	588.89	0.1%	586.96	0.1%	0.3%	620.74	0.1%	615.59	0.1%
2000	530.33	0.0%	603.00	0.0%	2%	706.48	0.1%	702.56	0.1%	1%	747.49	0.1%	740.28	0.1%
5000	610.20	0.0%	715.10	0.0%										
10000	727.32	0.0%												

Muscle

**Table B.2.** Absorbed dose per unit fluence ( $\text{pGy cm}^2$ ) under PA geometry from monoenergetic protons for UFH/NCI in standing and sitting posture.

PA	Sitting phantom			Standing phantom			Sitting phantom			Standing phantom			
	Energy (MeV)	$D_{\gamma}/\phi$ (pGy cm $^2$ )	Relative error	$D_{\gamma}/\phi$ (pGy cm $^2$ )	Relative difference (RD)	$D_{\gamma}/\phi$ (pGy cm $^2$ )	Relative error	$D_{\gamma}/\phi$ (pGy cm $^2$ )	Relative difference (RD)	$D_{\gamma}/\phi$ (pGy cm $^2$ )	Relative error	$D_{\gamma}/\phi$ (pGy cm $^2$ )	Relative difference (RD)
2 <sup>5</sup>													
10	0.026	6.7%	0.024	7.8%	9%	0.0154	2.3%	0.0155	2.6%	-1%	0.0034	5.4%	3%
20	0.064	4.7%	0.060	5.4%	7%	0.044	1.6%	0.043	1.8%	2%	0.0072	3.4%	0.0017
30	0.33	9.1%	0.28	8.2%	20%	75.46	0.1%	75.48	0.2%	0.0%	0.0167	2.5%	0.0171
50	2820.12	0.3%	2818.92	0.3%	0.0%	1133.12	0.1%	1134.15	0.1%	-0.1%	0.106	2.5%	0.105
100	1133.84	0.3%	1132.88	0.3%	0.1%	1271.32	0.1%	1271.46	0.1%	0.0%	1.39	1.4%	1.39
150	889.58	0.3%	887.28	0.3%	0.3%	898.51	0.1%	899.00	0.1%	-0.1%	960.86	0.1%	959.94
200	581.26	0.4%	577.48	0.4%	1%	555.03	0.1%	555.24	0.1%	0.0%	1146.57	0.1%	1145.81
500	547.28	0.5%	548.31	0.6%	-0.2%	519.26	0.1%	519.70	0.1%	-0.1%	615.62	0.1%	616.04
1000	548.01	0.6%	547.22	0.7%	0.1%	520.34	0.1%	520.22	0.1%	0.0%	580.13	0.1%	580.83
2000	603.95	0.7%	605.65	0.8%	-0.3%	593.21	0.1%	593.72	0.1%	-0.1%	570.41	0.1%	567.98
5000	720.31	1.0%	733.27	1.0%	-2%	705.10	0.1%	706.74	0.2%	-0.2%	649.98	0.1%	649.02
10000											765.26	0.2%	763.79
PA	Sitting phantom			Standing phantom			Sitting phantom			Standing phantom			
2 <sup>5</sup>													
10	0.00330	4.4%	0.00334	5.0%	-1%	0.018	5.0%	0.019	5.7%	-6%	0.0157	6.6%	0.0156
20	0.013	2.2%	0.014	2.4%	-8%	0.05	3.4%	0.04	3.9%	4%	0.04	8.7%	0.03
30	0.032	1.8%	0.033	1.8%	-3%	0.25	4.4%	0.27	5.8%	-8%	6.1%	18%	
50	0.17	2.1%	0.19	2.4%	-7%	100.33	0.2%	102.18	0.8%	-2%	2.37	5.2%	
100	80.47	0.3%	80.34	0.3%	0.2%	1240.91	0.1%	1291.43	0.1%	1287.23	0.2%	1665.85	0.2%
150	1241.28	0.1%	1240.91	0.1%	0.0%	933.52	0.2%	933.30	0.2%	0.0%	971.21	0.3%	
200	1004.88	0.1%	1004.81	0.1%	0.0%	593.44	0.2%	590.25	0.2%	1%	605.25	0.3%	
500	600.76	0.1%	602.50	0.1%	-0.3%	557.02	0.3%	555.70	0.3%	0.2%	574.42	0.5%	
1000	573.41	0.1%	576.38	0.1%	-1%	557.13	0.4%	557.96	0.4%	-0.1%	573.13	0.5%	
2000	575.41	0.1%	576.75	0.1%	-0.2%	618.16	0.4%	623.74	0.5%	-1%	573.35	0.7%	
5000	644.78	0.1%	643.60	0.2%	0.2%	743.25	0.5%	742.29	0.6%	0.1%	637.27	0.7%	
10000	773.77	0.2%	773.10	0.2%	0.1%						763.70	0.7%	766.14

**Table B.2.** (Continued)

PA	Sitting phantom			Standing phantom			Sitting phantom			Standing phantom					
	Energy (MeV)	$D_{T/\Phi}$ (pGy cm <sup>2</sup> )	Relative error	$D_{T/\Phi}$ (pGy cm <sup>2</sup> )	Relative difference (RD)	$D_{T/\Phi}$ (pGy cm <sup>2</sup> )	relative error	$D_{T/\Phi}$ (pGy cm <sup>2</sup> )	Relative difference (RD)	$D_{T/\Phi}$ (pGy cm <sup>2</sup> )	relative error	$D_{T/\Phi}$ (pGy cm <sup>2</sup> )	Relative difference (RD)		
Heart	2 <sup>5</sup>	10	0.0031	6.4%	0.0029	7.0%	8%	0.007	4.7%	0.008	5.2%	-4%	0.0038	4.7%	
	20	0.013	3.1%	0.012	3.6%	5%	0.032	2.3%	0.035	2.6%	-7%	0.017	2.0%	0.018	2.3%
	30	0.0315	2.4%	0.0325	3.2%	-3%	0.078	1.6%	0.084	2.2%	-7%	0.039	1.5%	0.039	1.7%
	50	0.17	2.4%	0.18	2.8%	-6%	464.55	0.1%	464.53	0.2%	0.0%	0.20	1.2%	0.21	1.3%
	100	34.11	0.4%	54.05	0.4%	0.1%	1691.84	0.1%	1692.59	0.1%	0.0%	483.72	0.1%	484.81	0.1%
	150	1362.87	0.1%	1368.38	0.1%	-0.4%	1035.80	0.1%	1035.95	0.1%	0.0%	1294.39	0.1%	1297.95	0.1%
	200	906.63	0.1%	994.73	0.1%	0.2%	837.54	0.1%	838.63	0.1%	-0.1%	972.34	0.1%	975.19	0.1%
	500	566.04	0.1%	596.44	0.1%	-0.1%	548.37	0.1%	549.83	0.1%	-0.3%	593.22	0.1%	595.56	0.1%
	1000	567.51	0.1%	568.85	0.2%	-0.2%	518.98	0.2%	520.68	0.2%	-0.3%	566.29	0.1%	569.38	0.1%
	2000	568.05	0.2%	569.18	0.2%	-0.2%	520.53	0.2%	522.54	0.2%	-0.4%	567.20	0.1%	568.66	0.1%
Lungs	5000	636.43	0.2%	637.12	0.2%	-0.1%	589.67	0.2%	591.25	0.2%	-0.3%	634.30	0.1%	634.53	0.1%
	10000	764.09	0.2%	763.19	0.2%	0.1%	696.73	0.2%	696.84	0.3%	0.0%	760.11	0.1%	760.19	0.1%
	2 <sup>5</sup>	PA	Sitting phantom	Standing phantom		Sitting phantom		Sitting phantom		Sitting phantom		Sitting phantom		Sitting phantom	
	10	0.00404	3.1%	0.00400	3.5%	1%	0.0112	8.0%	0.0108	8.7%	3%	0.0112	7.4%	0.0106	9.1%
	20	0.0186	1.5%	0.0190	1.7%	-2%	0.033	5.9%	0.027	6.4%	22%	0.029	6.7%	0.031	6.1%
Larynx	30	0.04	1.1%	0.05	1.3%	-2%	0.18	6.9%	0.17	8.4%	6%	0.20	6.2%	0.21	6.2%
	50	1.41	0.8%	1.40	0.9%	1%	149.32	0.6%	149.15	0.6%	0.1%	516.44	0.3%	515.70	0.3%
	100	1576.45	0.1%	1576.37	0.1%	0.0%	1317.09	0.2%	1325.08	0.2%	-1%	1323.95	0.2%	1317.42	0.2%
	150	1179.35	0.1%	1179.22	0.1%	0.0%	952.15	0.2%	955.91	0.2%	-0.4%	927.55	0.2%	923.51	0.2%
	200	890.28	0.1%	890.02	0.1%	0.0%	577.83	0.1%	577.05	0.3%	0.0%	589.56	0.2%	587.92	0.3%
	500	577.59	0.1%	577.83	0.1%	0.0%	543.95	0.4%	545.58	0.4%	-0.3%	548.78	0.3%	549.63	0.3%
	1000	540.27	0.1%	539.73	0.1%	0.1%	541.50	0.4%	545.74	0.5%	-1%	547.47	0.4%	548.12	0.4%
	2000	546.08	0.1%	545.70	0.1%	0.1%	613.94	0.6%	614.08	0.5%	0.0%	614.39	0.4%	612.91	0.5%
	5000	616.37	0.1%	615.56	0.1%	0.1%	734.12	0.1%	733.44	0.6%	0.1%	732.80	0.5%	728.70	0.5%
	10000	736.20	0.1%	735.83	0.1%										

(Continued)

**Table B.2.** (Continued)

PA	Sitting phantom			Standing phantom			Sitting phantom			Standing phantom				
	Energy (MeV)	$D_{T/\phi}$ (pGy cm <sup>2</sup> )	Relative error	$D_{T/\phi}$ (pGy cm <sup>2</sup> )	Relative difference (RD)	$D_{T/\phi}$ (pGy cm <sup>2</sup> )	Relative error	$D_{T/\phi}$ (pGy cm <sup>2</sup> )	Relative difference (RD)	$D_{T/\phi}$ (pGy cm <sup>2</sup> )	Relative error	$D_{T/\phi}$ (pGy cm <sup>2</sup> )	Relative difference (RD)	
2	5													
10	0.04	12.4%	0.03	8.0%	22%	0.019	8.5%	0.005	9.0%	-14%	0.014	5.2%	0.013	6.2%
20	0.19	15.2%	0.15	5.8%	32%	0.046	4.1%	0.020	4.4%	-4%	0.04	7.8%	0.05	9.3%
30	0.99	254.46	0.3%	2233.25	0.3%	537.35	0.2%	536.90	0.2%	3.2%	0.045	3%	0.04	9%
50	5.00	63.88	0.7%	569.31	0.7%	1268.89	0.1%	1269.51	0.1%	0.1%	0.04	1.7%	7.04	2.0%
100	1.91	1.91	2.21	7.2%	-13%	926.40	0.1%	924.86	0.1%	0.2%	1894.25	0.2%	1782.43	0.2%
150	999.95	0.3%	1005.86	0.4%	-1%	601.43	0.5%	596.42	0.2%	597.87	0.2%	572.34	0.2%	1143.06
200	500.00	0.4%	575.97	0.6%	-2%	563.64	0.2%	565.54	0.2%	-0.2%	879.82	0.2%	878.25	0.2%
500	1000.00	0.6%	574.37	0.7%	-1%	564.52	0.3%	566.64	0.3%	-0.4%	529.77	0.3%	571.86	0.2%
1000	571.21	0.7%	569.31	0.7%	1%	628.16	0.3%	626.78	0.3%	0.2%	505.64	0.3%	593.37	0.4%
2000	5000.00	0.7%	643.25	0.8%	0.1%	752.18	0.3%	753.91	0.4%	-0.2%	702.65	0.4%	696.88	0.4%
5000	10000.00	0.8%	774.52	0.8%	-0.3%									1%
10000	772.54													
PA	Sitting phantom			Standing phantom			Sitting phantom			Standing phantom			Standing phantom	
2	5													
10	0.003	4.0%	0.004	4.4%	-8%	703.74	0.0%	834.90	0.0%	-16%	0.0059	7.5%	0.0064	8.1%
20	0.014	2.0%	0.016	2.1%	-12%	1403.46	0.0%	1665.28	0.0%	-16%	0.027	3.5%	0.026	4.0%
30	0.03	1.7%	0.04	1.7%	-4%	1778.25	0.0%	2137.78	0.0%	-17%	0.064	2.9%	0.066	3.2%
50	0.18	1.6%	0.19	1.6%	-2%	1347.49	0.0%	1655.32	0.0%	-19%	6.04	1.2%	6.04	1.3%
100	202.78	0.1%	203.46	0.2%	-0.3%	980.37	0.0%	1238.67	0.0%	-21%	1880.15	0.2%	1885.22	0.2%
150	1461.53	0.1%	1461.60	0.1%	0.0%	837.30	0.0%	1057.32	0.0%	-21%	1086.11	0.2%	1091.27	0.2%
200	993.36	0.1%	993.98	0.1%	-0.1%	792.44	0.0%	950.04	0.0%	-17%	860.55	0.2%	863.94	0.2%
500	600.67	0.1%	603.25	0.1%	-0.4%	835.93	0.0%	881.10	0.0%	-5%	561.75	0.2%	565.41	0.2%
1000	573.70	0.1%	576.94	0.1%	-1%	529.03	0.0%	529.58	0.0%	-0.1%	531.61	0.2%	537.75	0.3%
2000	574.74	0.1%	578.51	0.1%	-1%	487.22	0.0%	486.55	0.0%	0.1%	530.28	0.3%	533.47	0.3%
5000	644.67	0.1%	644.90	0.1%	0.0%	480.22	0.0%	477.46	0.0%	1%	597.62	0.3%	599.65	0.3%
10000	773.04	0.1%	773.83	0.2%	-0.1%	561.38	0.0%	552.00	0.1%	2%	711.18	0.3%	714.92	0.4%

(Continued)

**Table B.2.** (*Continued*)

PA	Sitting phantom			Standing phantom			Sitting phantom			Standing phantom							
	Energy (MeV)	$D_{T/\phi}$ (pGy cm <sup>2</sup> )	Relative error														
Stomach	2 <sup>5</sup>	10	0.0034	7.0%	0.0034	8.3%	-0.5%	0.014	8.6%	0.012	9.6%	16%	0.013	8.6%	0.011	10.4%	14%
	20	0.0139	3.5%	0.0136	4.0%	2%	0.030	6.2%	0.032	7.2%	-6%	0.028	5.9%	0.029	7.2%	-3%	
	30	0.034	2.7%	0.032	3.3%	6%	0.19	3.3%	0.20	8.0%	0.18	12.3%	7%	0.18	6.0%	0.20	12.4%
	50	0.20	3.5%	0.19	3.3%	5%	2.11	4.7%	1.95	4.9%	8%	2.96	4.7%	5.61	4.8%	-47%	
	100	66.09	0.5%	65.70	0.5%	1%	1936.88	0.2%	1895.69	0.3%	2%	1439.51	0.2%	1455.22	0.3%	-1%	
	150	1546.17	0.1%	1542.17	0.1%	0.3%	988.52	0.2%	979.45	0.3%	1%	941.73	0.3%	951.60	0.3%	-1%	
	200	977.87	0.1%	977.94	0.1%	0.0%	604.00	0.2%	585.90	0.3%	0.4%	579.22	0.4%	590.87	0.4%	-2%	
	500	601.14	0.1%	601.14	0.1%	0.2%	576.26	0.2%	553.65	0.4%	0.5%	546.90	0.5%	554.84	0.5%	-2%	
	1000	572.05	0.2%	575.48	0.2%	-0.5%	558.16	0.5%	549.57	0.6%	2%	547.15	0.6%	556.64	0.7%	-2%	
	2000	572.72	0.2%	575.48	0.2%	-0.5%	625.78	0.6%	617.15	0.7%	1%	616.95	0.6%	623.31	0.7%	-1%	
Tonsil	5000	638.08	0.2%	640.70	0.3%	-0.4%	767.23	0.3%	751.77	0.7%	0.7%	736.00	0.7%	736.75	0.7%	0.1%	
	10000	764.81	0.3%														
	2 <sup>5</sup>	PA	Sitting phantom	Sitting phantom	Sitting phantom	Sitting phantom	Sitting phantom	Sitting phantom	Sitting phantom								
	5	10	0.0029	10.1%	0.0032	10.5%	-11%	0.0032	10.9%	0.0032	10.9%	0.0044	11.8%	-29%			
	20	0.012	5.1%	0.013	5.4%	-4%	0.014	5.2%	0.014	5.2%	0.018	5.6%	-25%				
Larynx	30	0.05	9.7%	0.04	11.1%	39%	0.030	5.2%	0.032	3.8%	-6%	0.034	4.2%	0.041	4.6%	-17%	
	50	0.26	13.9%	0.25	10.0%	0.13	0.16	2.6%	0.15	4.4%	-17%	0.19	4.0%	0.21	4.6%	-12%	
	100	272.10	0.5%	2718.93	0.6%	0.1%	1.66	3.3%	1.97	3.5%	-16%	2.01	2.4%	2.27	2.5%	-11%	
	150	1162.74	0.5%	1159.65	0.6%	0.3%	1301.48	0.2%	1303.18	0.2%	-0.1%	1613.82	0.1%	1616.93	0.2%	-0.2%	
	200	895.99	0.5%	892.53	0.6%	0.4%	1034.36	0.1%	1037.32	0.2%	-0.3%	969.09	0.2%	971.68	0.2%	-0.3%	
	500	581.39	0.7%	576.58	0.8%	1%	589.80	0.2%	599.03	0.2%	-2%	592.80	0.2%	597.55	0.2%	-1%	
	1000	546.37	0.9%	548.37	1.1%	-0.4%	566.24	0.3%	576.33	0.3%	-2%	562.11	0.3%	570.23	0.3%	-1%	
	2000	546.09	1.2%	543.66	1.4%	0.4%	570.90	0.3%	574.35	0.3%	-1%	564.06	0.3%	570.13	0.3%	-1%	
	5000	609.73	1.4%	607.83	1.5%	0.3%	646.48	0.4%	646.73	0.4%	0.0%	630.28	0.3%	637.33	0.4%	-1%	
	10000	747.55	3.0%	746.91	3.6%	0.1%	773.25	0.4%	781.35	0.5%	-1%	754.36	0.4%	763.38	0.4%	-1%	

(Continued)

**Table B.2.** (Continued)

PA	Sitting phantom			Standing phantom			Sitting phantom			Standing phantom				
	Energy (MeV)	$D_{T/\phi}$ (pGy cm <sup>2</sup> )	Relative error	$D_{T/\phi}$ (pGy cm <sup>2</sup> )	Relative difference (RD)	$D_{T/\phi}$ (pGy cm <sup>2</sup> )	Relative error	$D_{T/\phi}$ (pGy cm <sup>2</sup> )	Relative difference (RD)	$D_{T/\phi}$ (pGy cm <sup>2</sup> )	Relative error	$D_{T/\phi}$ (pGy cm <sup>2</sup> )	Relative difference (RD)	
<b>MUSCLE</b>														
2	0.0007	2.8%	0.0008	2.9%	-12%									
5	0.011	1.0%	0.013	1.1%	-13%									
10	0.08	0.5%	0.09	0.6%	-12%	0.007	3.9%	0.005	3.0%	40%	0.0051	2.2%	0.0052	2.5%
20	21.02	0.0%	27.78	0.0%	-24%	2.17	0.4%	1.22	0.6%	78%	0.551	1.0%	0.551	1.0%
30	64.49	0.0%	84.10	0.0%	-23%	29.17	0.1%	29.82	0.2%	-2%	12.69	0.2%	12.74	0.2%
50	305.44	0.0%	448.33	0.0%	-18%	248.35	0.1%	257.08	0.1%	-3%	153.26	0.1%	153.56	0.1%
100	918.54	0.0%	1154.38	0.0%	-20%	842.75	0.0%	1345.76	0.0%	-37%	1148.33	0.0%	1186.22	0.0%
150	966.00	0.0%	1117.08	0.0%	-14%	907.85	0.0%	1166.97	0.0%	-22%	1191.90	0.0%	1212.62	0.0%
200	868.92	0.0%	895.40	0.0%	-3%	724.67	0.0%	883.99	0.0%	-18%	903.30	0.0%	905.98	0.0%
500	561.40	0.0%	561.21	0.0%	0.0%	541.03	0.0%	557.06	0.0%	-3%	567.18	0.0%	573.13	0.0%
1000	528.77	0.0%	527.64	0.0%	0.2%	510.65	0.0%	525.86	0.0%	-3%	538.39	0.0%	544.02	0.1%
2000	529.76	0.0%	527.28	0.0%	0.5%	512.52	0.1%	521.26	0.1%	-2%	535.90	0.1%	540.89	0.1%
5000	607.54	0.0%	598.62	0.0%	1%	585.11	0.1%	580.60	0.1%	1%	594.17	0.1%	598.29	0.1%
10000	722.01	0.0%	709.26	0.0%	2%	705.15	0.1%	695.22	0.1%	1%	714.09	0.1%	719.04	0.1%

**Table B.3.** Absorbed dose per unit fluence ( $\text{pGy cm}^2$ ) under RLAT geometry from monoenergetic protons for UFH/NCI in standing and sitting posture.

RLAT	Sitting phantom			Standing phantom			Sitting phantom			Standing phantom		
	Energy (MeV)	$D_{\gamma}/\phi$ ( $\text{pGy cm}^2$ )	Relative error	$D_{\gamma}/\phi$ ( $\text{pGy cm}^2$ )								
2 <sup>5</sup>												
10	0.003	6.8%	0.002	5.3%	19%							
20	0.011	3.2%	0.010	2.6%	4%							
30	0.03	2.3%	0.02	1.9%	8%							
50	0.15	2.7%	0.14	1.9%	7%							
100	293.07	0.2%	286.13	0.2%	2%							
150	805.59	0.1%	1029.15	0.1%	-22%							
200	1048.04	0.1%	963.75	0.1%	9%							
500	585.09	0.1%	586.30	0.1%	-0.2%							
1000	559.74	0.1%	559.92	0.1%	0.0%							
2000	561.77	0.2%	562.69	0.1%	-0.2%							
5000	640.91	0.2%	642.33	0.1%	-0.2%							
10000	770.70	0.2%	769.26	0.2%	0.2%							
RLAT	Sitting phantom			Standing phantom			Sitting phantom			Standing phantom		
2 <sup>5</sup>												
10	0.003	6.8%	0.002	5.3%	19%							
20	0.011	3.2%	0.010	2.6%	4%							
30	0.03	2.3%	0.02	1.9%	8%							
50	0.15	2.7%	0.14	1.9%	7%							
100	293.07	0.2%	286.13	0.2%	2%							
150	805.59	0.1%	1029.15	0.1%	-22%							
200	1048.04	0.1%	963.75	0.1%	9%							
500	585.09	0.1%	586.30	0.1%	-0.2%							
1000	559.74	0.1%	559.92	0.1%	0.0%							
2000	561.77	0.2%	562.69	0.1%	-0.2%							
5000	640.91	0.2%	642.33	0.1%	-0.2%							
10000	770.70	0.2%	769.26	0.2%	0.2%							

(Continued)

**Table B.3.** (Continued)

RLAT		Sitting phantom			Standing phantom			Sitting phantom			Standing phantom			
Energy (MeV)	$D_{\gamma}/\phi$ (pGy cm <sup>2</sup> )	Relative error												
Heart	5	0.0013	10.5%	0.0014	8.2%	-6%	0.003	10.0%	0.002	7.9%	0.0032	5.5%	0.0032	4.1%
	10	0.0075	5.2%	0.0069	3.8%	8%	0.012	4.4%	0.011	3.7%	0.015	2.6%	0.013	2.1%
	20	0.019	3.6%	0.018	3.1%	7%	0.032	3.2%	0.027	2.8%	0.04	1.9%	0.03	1.5%
	30	0.109	4.1%	0.108	2.9%	1%	0.234	0.5%	0.234	0.4%	-0.2%	0.23	0.47	0.9%
	50	3.74	1.4%	4.42	1.0%	-15%	992.98	0.2%	527.88	0.2%	88%	412.76	0.1%	-17%
	100	983.01	0.2%	1103.22	0.1%	-11%	750.04	0.2%	791.07	0.1%	-5%	1201.77	0.1%	-2%
	200	1081.42	0.1%	1051.48	0.1%	3%	981.96	0.2%	1092.62	0.1%	-10%	1008.87	0.1%	3%
	500	588.04	0.1%	590.22	0.1%	-0.4%	586.04	0.2%	579.43	0.1%	1%	575.40	0.1%	-1%
	1000	564.65	0.2%	565.33	0.1%	-0.1%	559.92	0.2%	552.68	0.2%	1%	547.56	0.1%	-1%
	2000	566.87	0.2%	566.33	0.2%	0.1%	557.30	0.2%	555.62	0.2%	0.3%	551.88	0.1%	-0.1%
Lungs	5000	647.46	0.2%	645.12	0.2%	0.4%	632.27	0.2%	638.32	0.2%	-1%	626.14	0.1%	-0.1%
	10000	775.69	0.3%	772.30	0.2%	0.4%	751.30	0.3%	760.17	0.2%	-1%	750.61	0.2%	0.1%
RLAT		Sitting phantom			Standing phantom			Sitting phantom			Standing phantom			
Energy (MeV)	$D_{\gamma}/\phi$ (pGy cm <sup>2</sup> )	Relative error												
Extro-thoracic region	5	0.002	4.9%	0.002	3.7%	0.0%	26.42	1.3%	26.25	1.0%	1%	0.016	7.2%	0.019
	10	0.0107	2.3%	0.0105	1.8%	2%	70.06	1.0%	69.27	0.8%	1%	0.064	8.3%	0.057
	20	0.0263	1.8%	0.0258	1.4%	2%	140.05	0.6%	139.56	0.5%	0.4%	23.80	1.1%	5.0%
	30	0.139	1.7%	0.143	1.4%	-3%	1890.00	0.2%	1887.83	0.2%	0%	2121.97	0.2%	-2%
	50	316.59	0.1%	379.41	0.1%	-17%	1081.62	0.2%	1082.10	0.2%	0%	1075.50	0.2%	0%
	100	900.21	0.1%	896.04	0.1%	0.5%	863.72	0.2%	862.15	0.2%	0.2%	859.92	0.2%	0.1%
	200	1061.27	0.1%	1057.55	0.1%	0.4%	569.54	0.3%	568.27	0.2%	0.2%	565.77	0.3%	0.2%
	500	567.74	0.1%	566.45	0.1%	0.2%	532.46	0.4%	534.90	0.3%	-0.5%	533.74	0.4%	0.3%
	1000	533.00	0.1%	532.07	0.1%	0.2%	529.07	0.5%	531.72	0.4%	-0.5%	530.95	0.4%	0.0%
	2000	542.72	0.1%	541.13	0.1%	0.3%	590.42	0.6%	600.88	0.5%	-2%	593.91	0.5%	0.4%
Oral mucosa	5000	628.63	0.1%	626.72	0.1%	0.3%	700.71	0.6%	712.83	0.6%	-2%	703.79	0.5%	0.4%
	10000	754.91	0.1%	753.07	0.1%	0.2%						704.19	0.4%	-0.1%

(Continued)

**Table B.3.** (*Continued*)

RLAT	Sitting phantom			Standing phantom			Sitting phantom			Standing phantom								
	Energy (MeV)	$D_{\gamma}/\phi$ (pGy cm <sup>2</sup> )	Relative error	$D_{\gamma}/\phi$ (pGy cm <sup>2</sup> )														
Ovaries	2	5	10	0.021	10.1%	0.015	9.8%	39%	0.0065	8.1%	0.0072	6.0%	-9%	83.06	0.5%	83.39	0.4%	-0.4%
	20	0.11	8.6%	0.13	14.8%	-11%	0.018	5.7%	0.017	5.0%	0.017	5.0%	6%	393.21	0.3%	396.39	0.2%	-1%
	30	0.09	0.7%	24.33	2.7%	3637%	401.05	0.4%	9.47	1.4%	4137%	1145.56	0.2%	1222.82	0.2%	-2%	-3%	
	50	1140.91	0.6%	1421.47	0.5%	-20%	1226.48	0.3%	1094.88	0.2%	12%	869.20	0.2%	1147.60	0.2%	-0.2%	-0.2%	
	500	601.21	0.6%	569.77	0.5%	6%	597.90	0.3%	574.55	0.2%	4%	563.08	0.3%	564.31	0.2%	-0.2%	-0.2%	
	1000	575.36	0.7%	552.81	0.6%	4%	575.82	0.3%	552.29	0.2%	4%	524.85	0.3%	525.37	0.3%	-0.1%	-0.1%	
	2000	577.14	0.9%	555.94	0.7%	4%	577.84	0.3%	558.96	0.3%	3%	521.07	0.4%	521.01	0.3%	0.0%	0.0%	
	5000	649.86	0.9%	643.82	0.7%	1%	661.59	0.4%	647.39	0.3%	2%	588.14	0.4%	588.83	0.3%	-0.1%	-0.1%	
	10000	782.00	1.0%	778.18	0.7%	0.5%	796.22	0.4%	785.22	0.3%	1%	692.61	0.5%	693.26	0.4%	-0.1%	-0.1%	
	RLAT	Sitting phantom			Standing phantom			Sitting phantom			Standing phantom							
Small intestine	2	5	10	0.003	5.9%	0.002	4.7%	21%	230.34	0.0%	199.56	0.0%	15%					
	20	0.011	2.9%	0.009	2.3%	22%	1146.36	0.0%	993.29	0.0%	15%							
	30	0.03	2.1%	0.02	1.9%	17%	1475.62	0.0%	1320.55	0.0%	12%	0.0040	8.9%	0.0037	6.7%	8%		
	50	3.13	0.9%	0.13	1.8%	2389%	1139.14	0.0%	1070.12	0.0%	6%	0.0092	6.6%	0.0092	5.3%	-0.1%		
	100	348.62	0.2%	158.98	0.2%	119%	880.26	0.0%	855.61	0.0%	2%	0.063	7.3%	0.061	6.2%	3%		
	150	1048.39	0.1%	832.08	0.1%	26%	882.69	0.0%	840.51	0.0%	3%	0.93	4.1%	0.82	3.2%	13%		
	200	1050.06	0.1%	1118.30	0.1%	-6%	803.01	0.0%	769.91	0.0%	5%	3.84	2.5%	3.32	2.0%	16%		
	500	597.36	0.1%	584.87	0.1%	2%	525.81	0.0%	522.52	0.0%	4%	742.41	0.2%	184.28	0.3%	303%		
	1000	571.65	0.1%	560.77	0.1%	2%	484.21	0.0%	480.82	0.0%	1%	563.08	0.3%	543.40	0.2%	4%		
	2000	572.51	0.1%	564.75	0.1%	1%	478.32	0.1%	475.30	0.0%	1%	567.05	0.3%	554.51	0.2%	2%		
	5000	646.40	0.2%	644.90	0.1%	0.2%	558.94	0.1%	558.60	0.0%	0.1%	666.74	0.3%	653.85	0.2%	2%		
	10000	774.49	0.2%	773.52	0.1%	0.1%	649.76	0.1%	648.98	0.0%	0.1%	801.23	0.3%	794.50	0.2%	1%		

(Continued)

**Table B.3.** (Continued)

RLAT		Sitting phantom		Standing phantom		Sitting phantom		Standing phantom		Sitting phantom		Standing phantom	
Energy (MeV)	$D_{\gamma}/\phi$ (pGy cm <sup>2</sup> )	Relative error											
Stomach	2	5	10	0.0050	6.7%	0.0054	5.5%	-8%	0.024	9.6%	0.023	7.0%	6%
	20	0.0134	4.8%	0.0131	8.6%	0.0131	4.3%	2%	0.16	14.7%	0.13	9.0%	23%
	30	0.09	7.2%	0.07	4.3%	0.07	22%						
	50	1.03	3.1%	1.05	2.5%	1.05	1.95	7.2%	1.96	5.2%	-1%	122.89	1.1%
	100	43.64	0.6%	114.53	0.3%	114.53	62%	-1%	1709.93	0.4%	1670.19	0.3%	Thyroid
	150	904.82	0.2%	1218.21	0.1%	1218.21	-26%	-26%	971.50	0.4%	966.02	0.3%	
	200	500	587.63	0.2%	595.34	0.1%	-1%	-1%	573.48	0.5%	569.73	0.3%	
	1000	566.43	0.2%	575.38	0.2%	-2%	-2%	-2%	540.49	0.6%	539.35	0.4%	
	2000	573.15	0.3%	577.04	0.2%	-1%	-1%	-1%	552.47	0.7%	545.43	0.5%	
	5000	665.59	0.3%	671.12	0.2%	-1%	-1%	-1%	622.71	0.8%	617.24	0.6%	
RLAT	10000	802.52	0.3%	803.08	0.2%	-0.1%	-0.1%	-0.1%	738.34	0.8%	730.94	0.6%	
	2	5	10	0.04	10.8%	0.05	8.5%	-16%	0.008	7.3%	0.007	5.8%	25%
	20	0.04	10.8%	0.05	8.5%	0.05	8.5%	-16%	0.022	5.0%	0.018	7.7%	24%
	30	0.122.56	0.8%	1122.24	0.6%	1122.24	0.6%	-3%	0.12	7.7%	0.11	7.4%	5%
	50	2193.19	0.9%	2254.17	0.6%	2254.17	0.6%	-3%	1.62	4.0%	1.20	3.4%	34%
	100	866.60	0.8%	874.94	0.6%	874.94	0.6%	-1%	894.40	0.3%	512.39	0.3%	75%
	150	571.20	1.0%	570.15	0.7%	570.15	0.7%	-0.2%	1083.86	0.2%	1272.44	0.2%	-15%
	200	553.13	1.3%	533.19	0.9%	533.19	0.9%	-4%	596.09	0.2%	579.40	0.2%	3%
	500	545.50	1.5%	527.08	1.1%	527.08	1.1%	-3%	574.25	0.3%	556.85	0.2%	3%
	10000	602.76	1.7%	583.56	1.2%	583.56	1.2%	-3%	650.12	0.4%	646.46	0.3%	1%
Tonsil	2	5	10	0.7%	697.81	1.7%	784.68	0.5%	784.68	0.5%	780.54	0.4%	1%
	20	0.531.13	1.3%	533.19	0.9%	533.19	0.9%	-4%	574.15	0.4%	560.61	0.3%	2%
	30	545.50	1.5%	527.08	1.1%	527.08	1.1%	-3%	650.12	0.4%	646.46	0.4%	1%
	50	602.76	1.7%	583.56	1.2%	583.56	1.2%	-3%	784.68	0.5%	780.54	0.4%	1%
	10000	715.86	1.7%	697.81	1.7%	697.81	1.7%	-3%	784.68	0.5%	780.54	0.4%	1%
	2	5	10	0.04	10.8%	0.05	8.5%	-16%	0.008	7.3%	0.007	5.8%	25%
	20	0.04	10.8%	0.05	8.5%	0.05	8.5%	-16%	0.022	5.0%	0.018	7.9%	0.008
	30	0.122.56	0.8%	1122.24	0.6%	1122.24	0.6%	-3%	0.12	7.7%	0.11	7.4%	0.007
	50	2193.19	0.9%	2254.17	0.6%	2254.17	0.6%	-3%	1.62	4.0%	1.20	3.4%	3.4%
	100	866.60	0.8%	874.94	0.6%	874.94	0.6%	-1%	894.40	0.3%	512.39	0.3%	75%
	150	571.20	1.0%	570.15	0.7%	570.15	0.7%	-0.2%	1083.86	0.2%	1272.44	0.2%	-15%
	200	553.13	1.3%	533.19	0.9%	533.19	0.9%	-4%	596.09	0.2%	579.40	0.2%	3%
	500	545.50	1.5%	527.08	1.1%	527.08	1.1%	-3%	574.25	0.3%	556.85	0.2%	3%
	10000	602.76	1.7%	583.56	1.2%	583.56	1.2%	-3%	650.12	0.4%	646.46	0.3%	1%
	2	5	10	0.04	10.8%	0.05	8.5%	-16%	0.008	7.3%	0.007	5.8%	25%
Uterus	20	0.04	10.8%	0.05	8.5%	0.05	8.5%	-16%	0.022	5.0%	0.018	7.9%	0.008
	30	0.122.56	0.8%	1122.24	0.6%	1122.24	0.6%	-3%	0.12	7.7%	0.11	7.4%	0.007
	50	2193.19	0.9%	2254.17	0.6%	2254.17	0.6%	-3%	1.62	4.0%	1.20	3.4%	3.4%
	100	866.60	0.8%	874.94	0.6%	874.94	0.6%	-1%	894.40	0.3%	512.39	0.3%	75%
	150	571.20	1.0%	570.15	0.7%	570.15	0.7%	-0.2%	1083.86	0.2%	1272.44	0.2%	-15%
	200	553.13	1.3%	533.19	0.9%	533.19	0.9%	-4%	596.09	0.2%	579.40	0.2%	3%
	500	545.50	1.5%	527.08	1.1%	527.08	1.1%	-3%	574.25	0.3%	556.85	0.2%	3%
	10000	602.76	1.7%	583.56	1.2%	583.56	1.2%	-3%	650.12	0.4%	646.46	0.3%	1%
	2	5	10	0.04	10.8%	0.05	8.5%	-16%	0.008	7.3%	0.007	5.8%	25%
	20	0.04	10.8%	0.05	8.5%	0.05	8.5%	-16%	0.022	5.0%	0.018	7.9%	0.008
Bladder	30	0.122.56	0.8%	1122.24	0.6%	1122.24	0.6%	-3%	0.12	7.7%	0.11	7.4%	0.007
	50	2193.19	0.9%	2254.17	0.6%	2254.17	0.6%	-3%	1.62	4.0%	1.20	3.4%	3.4%
	100	866.60	0.8%	874.94	0.6%	874.94	0.6%	-1%	894.40	0.3%	512.39	0.3%	75%
	150	571.20	1.0%	570.15	0.7%	570.15	0.7%	-0.2%	1083.86	0.2%	1272.44	0.2%	-15%
	200	553.13	1.3%	533.19	0.9%	533.19	0.9%	-4%	596.09	0.2%	579.40	0.2%	3%
	500	545.50	1.5%	527.08	1.1%	527.08	1.1%	-3%	574.25	0.3%	556.85	0.2%	3%
	10000	602.76	1.7%	583.56	1.2%	583.56	1.2%	-3%	650.12	0.4%	646.46	0.3%	1%
	2	5	10	0.04	10.8%	0.05	8.5%	-16%	0.008	7.3%	0.007	5.8%	25%
	20	0.04	10.8%	0.05	8.5%	0.05	8.5%	-16%	0.022	5.0%	0.018	7.9%	0.008
Lungs	30	0.122.56	0.8%	1122.24	0.6%	1122.24	0.6%	-3%	0.12	7.7%	0.11	7.4%	0.007
	50	2193.19	0.9%	2254.17	0.6%	2254.17	0.6%	-3%	1.62	4.0%	1.20	3.4%	3.4%
	100	866.60	0.8%	874.94	0.6%	874.94	0.6%	-1%	894.40	0.3%	512.39	0.3%	75%
	150	571.20	1.0%	570.15	0.7%	570.15	0.7%	-0.2%	1083.86	0.2%	1272.44	0.2%	-15%
	200	553.13	1.3%	533.19	0.9%	533.19	0.9%	-4%	596.09	0.2%	579.40	0.2%	3%
	500	545.50	1.5%	527.08	1.1%	527.08	1.1%	-3%	574.25	0.3%	556.85	0.2%	3%
	10000	602.76	1.7%	583.56	1.2%	583.56	1.2%	-3%	650.12	0.4%	646.46	0.3%	1%
	2	5	10	0.04	10.8%	0.05	8.5%	-16%	0.008	7.3%	0.007	5.8%	25%
	20	0.04	10.8%	0.05	8.5%	0.05	8.5%	-16%	0.022	5.0%	0.018	7.9%	0.008
Trachea	30	0.122.56	0.8%	1122.24	0.6%	1122.24	0.6%	-3%	0.12	7.7%	0.11	7.4%	0.007
	50	2193.19	0.9%	2254.17	0.6%	2254.17	0.6%	-3%	1.62	4.0%	1.20	3.4%	3.4%
	100	866.60	0.8%	874.94	0.6%	874.94	0.6%	-1%	894.40	0.3%	512.39	0.3%	75%
	150	571.20	1.0%	570.15	0.7%	570.15	0.7%	-0.2%	1083.86	0.2%	1272.44	0.2%	-15%
	200	553.13	1.3%	533.19	0.9%	533.19	0.9%	-4%	596.09	0.2%	579.40	0.2%	3%
	500	545.50	1.5%	527.08	1.1%	527.08	1.1%	-3%	574.25	0.3%	556.85	0.2%	3%
	10000	602.76	1.7%	583.56	1.2%	583.56	1.2%	-3%	650.12	0.4%	646.46	0.3%	1%
	2	5	10	0.04	10.8%	0.05	8.5%	-16%	0.008	7.3%	0.007	5.8%	25%
	20	0.04	10.8%	0.05	8.5%	0.05	8.5%	-16%	0.022	5.0%	0.018	7.9%	0.008
Uterus	30	0.122.56	0.8%	1122.24	0.6%	1122.24	0.6%	-3%	0.12	7.7%	0.11	7.4%	0.007
	50	2193.19	0.9%	2254.17	0.6%	2254.17	0.6%	-3%	1.62	4.0%	1.20	3.4%	3.4%
	100	866.60	0.8%	874.94	0.6%	874.94	0.6%	-1%	894.40	0.3%	512.39	0.3%	75%
	150	571.20	1.0%	570.15	0.7%	570.15	0.7%	-0.2%	1083.86	0.2%	1272.44	0.2%	-15%
	200	553.13	1.3%	533.19	0.9%	533.19	0.9%	-4%	596.09	0.2%	579.40	0.2%	3%
	500	545.50	1.5%	527.08	1.1%	527.08	1.1%	-3%	574.25	0.3%	556.85	0.2%	3%
	10000	602.76	1.7%	583.56	1.2%	583.56	1.2%	-3%	650.12	0.4%	646.46	0.3%	1%
	2	5	10	0.04	10.8%	0.05	8.5%	-1					

**Table B.3.** (*Continued*)

RLAT	Sitting phantom			Standing phantom			Sitting phantom			Standing phantom						
	Energy (MeV)	$D_{\gamma}/\phi$ (pGy cm <sup>2</sup> )	Relative error	$D_{\gamma}/\phi$ (pGy cm <sup>2</sup> )	Relative difference (RD)	$D_{\gamma}/\phi$ (pGy cm <sup>2</sup> )	Relative error	$D_{\gamma}/\phi$ (pGy cm <sup>2</sup> )	Relative difference (RD)	$D_{\gamma}/\phi$ (pGy cm <sup>2</sup> )	Relative error	$D_{\gamma}/\phi$ (pGy cm <sup>2</sup> )	Relative difference (RD)			
Muscle	2	0.00074	3.3%	0.00067	2.5%	12%										
	5	0.012	1.2%	0.011	0.9%	8%	0.001	3.4%	0.006	3.6%	-82%	0.002	3.6%	0.003	2.9%	
	10	0.08	0.6%	0.07	0.5%	8%	0.001	4.57	0.4%	5.21	0.3%	-12%	0.35	0.7%	0.38	0.5%
	20	31.10	0.0%	31.12	0.0%	-0.1%	35.03	0.2%	39.39	0.1%	-11%	9.04	0.2%	9.27	0.2%	
	30	88.18	0.0%	88.27	0.0%	-0.1%	252.86	0.1%	266.43	0.1%	-5%	98.75	0.1%	93.33	0.1%	
	50	264.29	0.0%	249.55	0.0%	6%	769.26	0.1%	710.14	0.0%	8%	449.19	0.1%	378.53	0.0%	
	100	693.57	0.0%	642.42	0.0%	8%	991.60	0.0%	902.27	0.0%	10%	992.83	0.0%	782.65	0.0%	
	150	879.04	0.0%	852.93	0.0%	3%	911.46	0.0%	871.71	0.0%	5%	1009.03	0.0%	969.77	0.0%	
	200	935.53	0.0%	911.46	0.0%	3%	551.69	0.0%	549.42	0.0%	0.4%	572.66	0.0%	569.27	0.0%	
	500	560.33	0.0%	556.68	0.0%	1%	522.80	0.1%	521.12	0.0%	0.3%	547.30	0.1%	545.42	0.0%	
	1000	528.62	0.0%	525.11	0.0%	1%	520.33	0.1%	519.86	0.0%	0.1%	545.43	0.1%	545.40	0.1%	
	2000	530.50	0.0%	527.91	0.0%	0.5%	589.04	0.1%	590.83	0.1%	-0.5%	614.73	0.1%	617.40	0.1%	
	5000	611.32	0.0%	611.24	0.0%	0.0%	706.82	0.1%	709.52	0.1%	-0.4%	739.46	0.1%	744.87	0.1%	
	10 000	727.87	0.0%	728.09	0.0%											

**Table B.4.** Absorbed dose per unit fluence ( $\text{pGy cm}^2$ ) under LLAT geometry from monoenergetic protons for UFH/NCI in standing and sitting posture.

LLAT	Sitting phantom			Standing phantom			Sitting phantom			Standing phantom		
	Energy (MeV)	$D_{\gamma}/\phi$ ( $\text{pGy cm}^2$ )	Relative error	$D_{\gamma}/\phi$ ( $\text{pGy cm}^2$ )								
2	5											
10	0.003	6.7%	0.002	5.4%	19%	0.010	10.1%	0.009	6.7%	10%	0.0079	10.9%
20	0.011	3.0%	0.009	2.5%	20%	0.03	6.8%	0.02	4.6%	15%	0.0178	8.4%
30	0.03	2.4%	0.02	1.9%	15%	0.14	9.3%	0.13	6.5%	12%		
50	0.04	0.5%	0.14	2.3%	18.608%	0.26	126.79	1.0%	127.60	0.8%	1.20	8.4%
100	0.11	0.2%	0.05	0.2%	0.1%	0.16	789.86	0.4%	748.40	0.3%	22.39	3.1%
150	0.70	0.1%	934.87	0.1%	-16%	1033.51	0.2%	1041.68	0.2%	-1%	1479.00	0.4%
200	1053.51	0.1%	984.84	0.1%	7%	1033.51	0.2%	1041.68	0.2%	0%	1374.21	0.3%
500	585.86	0.1%	588.40	0.1%	-0.4%	567.57	0.3%	569.04	0.2%	0%	585.21	0.4%
1000	560.50	0.1%	561.27	0.1%	-0.1%	546.01	0.4%	545.53	0.3%	0%	560.67	0.6%
2000	562.02	0.2%	563.05	0.1%	-0.2%	550.36	0.5%	551.01	0.3%	0%	559.96	0.7%
5000	639.97	0.2%	643.11	0.1%	-0.5%	626.09	0.5%	626.41	0.4%	0%	654.70	0.8%
10000	769.90	0.2%	770.06	0.2%	0.0%	755.16	0.6%	755.69	0.4%	0%	788.82	0.8%
2	5											
10	0.003	5.2%	0.003	4.2%	11%	0.003	7.4%	0.003	5.7%	0.003	5.7%	0.00%
20	0.015	2.8%	0.015	2.0%	2%	0.020	3.4%	0.019	2.6%	0.019	2.6%	6%
30	0.046	1.8%	0.046	1.4%	1%	0.021	0.2%	0.024	0.2%	0.024	0.2%	-0.3%
50	0.13	41%	0.13	36.14	0.1%	0.136	0.1%	0.136	0.1%	0.136	0.1%	0.1%
100	1.73	13%	1.73	131.01	0.1%	1.73	131.84	0.1%	0.1%	0.1%	0.1%	0.1%
150	1046.89	0.4%	113.83	1.0%	820%	0.1%	1187.37	0.1%	0%	927.48	0.2%	922.47
200	1012.00	0.4%	1353.61	0.3%	-25%	883.18	0.1%	884.31	0.1%	0%	982.38	0.2%
500	604.89	0.5%	569.10	0.4%	6%	560.15	0.1%	560.57	0.1%	0%	558.43	0.2%
1000	581.74	0.6%	550.99	0.5%	6%	524.19	0.1%	524.67	0.1%	0%	518.75	0.2%
2000	576.62	0.7%	552.97	0.6%	4%	522.84	0.1%	523.73	0.1%	0%	514.51	0.2%
5000	654.73	0.8%	635.17	0.7%	3%	592.52	0.1%	593.50	0.1%	0%	594.97	0.2%
10000	771.81	0.8%	767.48	0.7%	1%	704.34	0.2%	705.44	0.1%	0%	696.05	0.2%
2	5											
10	0.003	5.2%	0.003	4.2%	11%	0.003	7.4%	0.003	5.7%	0.003	5.7%	0.00%
20	0.015	2.8%	0.015	2.0%	2%	0.020	3.4%	0.019	2.6%	0.019	2.6%	6%
30	0.046	1.8%	0.046	1.4%	1%	0.021	0.2%	0.024	0.2%	0.024	0.2%	-0.3%
50	0.13	41%	0.13	136.32	0.1%	0.136	0.1%	0.136	0.1%	0.136	0.1%	0.1%
100	1.73	13%	1.73	131.84	0.1%	1.73	131.84	0.1%	0%	0.153	0.2%	0.154%
150	1046.89	0.4%	113.83	1.0%	820%	0.1%	1187.37	0.1%	0%	927.48	0.2%	922.47
200	1012.00	0.4%	1353.61	0.3%	-25%	883.18	0.1%	884.31	0.1%	0%	982.38	0.2%
500	604.89	0.5%	569.10	0.4%	6%	560.15	0.1%	560.57	0.1%	0%	554.60	0.2%
1000	581.74	0.6%	550.99	0.5%	6%	524.19	0.1%	524.67	0.1%	0%	513.89	0.2%
2000	576.62	0.7%	552.97	0.6%	4%	522.84	0.1%	523.73	0.1%	0%	514.51	0.2%
5000	654.73	0.8%	635.17	0.7%	3%	592.52	0.1%	593.50	0.1%	0%	594.97	0.2%
10000	771.81	0.8%	767.48	0.7%	1%	704.34	0.2%	705.44	0.1%	0%	691.57	0.2%
2	5											
10	0.003	5.2%	0.003	4.2%	11%	0.003	7.4%	0.003	5.7%	0.003	5.7%	0.00%
20	0.015	2.8%	0.015	2.0%	2%	0.020	3.4%	0.019	2.6%	0.019	2.6%	6%
30	0.046	1.8%	0.046	1.4%	1%	0.021	0.2%	0.024	0.2%	0.024	0.2%	-0.3%
50	0.13	41%	0.13	136.32	0.1%	0.136	0.1%	0.136	0.1%	0.136	0.1%	0.1%
100	1.73	13%	1.73	131.84	0.1%	1.73	131.84	0.1%	0%	0.153	0.2%	0.154%
150	1046.89	0.4%	113.83	1.0%	820%	0.1%	1187.37	0.1%	0%	927.48	0.2%	922.47
200	1012.00	0.4%	1353.61	0.3%	-25%	883.18	0.1%	884.31	0.1%	0%	982.38	0.2%
500	604.89	0.5%	569.10	0.4%	6%	560.15	0.1%	560.57	0.1%	0%	554.60	0.2%
1000	581.74	0.6%	550.99	0.5%	6%	524.19	0.1%	524.67	0.1%	0%	513.89	0.2%
2000	576.62	0.7%	552.97	0.6%	4%	522.84	0.1%	523.73	0.1%	0%	514.51	0.2%
5000	654.73	0.8%	635.17	0.7%	3%	592.52	0.1%	593.50	0.1%	0%	594.97	0.2%
10000	771.81	0.8%	767.48	0.7%	1%	704.34	0.2%	705.44	0.1%	0%	691.57	0.2%
2	5											
10	0.003	5.2%	0.003	4.2%	11%	0.003	7.4%	0.003	5.7%	0.003	5.7%	0.00%
20	0.015	2.8%	0.015	2.0%	2%	0.020	3.4%	0.019	2.6%	0.019	2.6%	6%
30	0.046	1.8%	0.046	1.4%	1%	0.021	0.2%	0.024	0.2%	0.024	0.2%	-0.3%
50	0.13	41%	0.13	136.32	0.1%	0.136	0.1%	0.136	0.1%	0.136	0.1%	0.1%
100	1.73	13%	1.73	131.84	0.1%	1.73	131.84	0.1%	0%	0.153	0.2%	0.154%
150	1046.89	0.4%	113.83	1.0%	820%	0.1%	1187.37	0.1%	0%	927.48	0.2%	922.47
200	1012.00	0.4%	1353.61	0.3%	-25%	883.18	0.1%	884.31	0.1%	0%	982.38	0.2%
500	604.89	0.5%	569.10	0.4%	6%	560.15	0.1%	560.57	0.1%	0%	554.60	0.2%
1000	581.74	0.6%	550.99	0.5%	6%	524.19	0.1%	524.67	0.1%	0%	513.89	0.2%
2000	576.62	0.7%	552.97	0.6%	4%	522.84	0.1%	523.73	0.1%	0%	514.51	0.2%
5000	654.73	0.8%	635.17	0.7%	3%	592.52	0.1%	593.50	0.1%	0%	594.97	0.2%
10000	771.81	0.8%	767.48	0.7%	1%	704.34	0.2%	705.44	0.1%	0%	691.57	0.2%
2	5											
10	0.003	5.2%	0.003	4.2%	11%	0.003	7.4%	0.003	5.7%	0.003	5.7%	0.00%
20	0.015	2.8%	0.015	2.0%	2%	0.020	3.4%	0.019	2.6%	0.019	2.6%	6%
30	0.046	1.8%	0.046	1.4%	1%	0.021	0.2%	0.024	0.2%	0.024	0.2%	-0.3%
50	0.13	41%	0.13	136.32	0.1%	0.136	0.1%	0.136	0.1%	0.136	0.1%	0.1%
100	1.73	13%	1.73	131.84	0.1%	1.73	131.84	0.1%	0%	0.153	0.2%	0.154%
150	1046.89	0.4%	113.83	1.0%	820%	0.1%	1187.37	0.1%	0%	927.48	0.2%	922.47
200	1012.00	0.4%	1353.61	0.3%	-25%	883.18	0.1%	884.31	0.1%	0%	982.38	0.2%
500	604.89	0.5%	569.10	0.4%	6%	560.15	0.1%	560.57	0.1%	0%	554.60	0.2%
1000	581.74	0.6%	550.99	0.5%	6%	524.19	0.1%	524.67	0.1%	0%	513.89	0.2%
2000	576.62	0.7%	552.97	0.6%	4%	522.84	0.1%	523.73	0.1%	0%	514.51	0.2%
5000	654.73	0.8%	635.17	0.7%	3%	592.52	0.1%	593.50	0.1%	0%	594.97	0.2%
10000	771.81	0.8%	767.48	0.7%	1%	704.34	0.2%	705.44	0.1%	0%	691.57	0.2%
2	5											
10	0.003	5.2%	0.003	4.2%	11%	0.003	7.4%	0.003	5.7%	0.003	5.7%	0.00%
20	0.015	2.8%	0.015	2.0%	2%	0.020	3.4%	0.019	2.6%	0.019	2.6%	6%
30	0.046	1.8%	0.046	1.4%	1%	0.021	0.2%	0.024	0.2%	0.024	0.2%	-0.3%
50	0.13	41%	0.13	136.32	0.1%	0.136	0.1%	0.136	0.1%	0.136	0.1%	0.1%
100	1.73	13%	1.73	131.84	0.1%	1.73	131.84	0.1%	0%	0.153	0.2%	0.154%
150	1046.89	0.4%	113.83	1.0%	820%	0.1%	1187.37	0.1%	0%	927.48	0.2%	922.47
200	1012.00	0.4%	1353.61	0.3%	-25%	883.18	0.1%	884.31	0.1%	0%	982.38	0.2%
500	604.89	0.5%	569.10	0.4%	6%	560.15	0.1%	560.57	0.1%	0%	554.60	0.2%
1000	581.74	0.6%	550.99	0.5%	6%	524.19	0.1%	524.67	0.1%	0%	513.89	0.2%
2000	576.62	0.7%	552.97</td									

**Table B.4.** (Continued)

LLAT		Sitting phantom		Standing phantom		Sitting phantom		Standing phantom		Sitting phantom		Standing phantom			
	Energy (MeV)	$D_{\gamma}\phi$ (pGy cm <sup>2</sup> )	Relative error	$D_{\gamma}\phi$ (pGy cm <sup>2</sup> )	Relative difference (RD)	$D_{\gamma}\phi$ (pGy cm <sup>2</sup> )	Relative error	$D_{\gamma}\phi$ (pGy cm <sup>2</sup> )	Relative difference (RD)	$D_{\gamma}\phi$ (pGy cm <sup>2</sup> )	Relative error	$D_{\gamma}\phi$ (pGy cm <sup>2</sup> )	Relative error		
Heart	5	0.003	8.9%	0.002	6.8%	0.0024	9.6%	0.0022	7.7%	8%	0.00131	8.2%	0.00133	6.3%	
	10	0.010	4.3%	0.011	3.3%	0.013	4.5%	0.010	3.6%	25%	0.0064	3.9%	0.0059	3.0%	
	20	0.029	3.0%	0.027	2.6%	0.031	3.4%	0.027	2.9%	18%	0.016	2.9%	0.014	2.2%	
	30	0.15	3.1%	0.16	2.7%	1.00	2.2%	0.95	1.7%	5%	0.091	2.4%	0.086	1.8%	
	50	321.75	0.2%	391.81	0.1%	-18%	998.70	0.2%	446.66	0.2%	124%	2.30	0.8%	6.20	0.5%
	100	1242.44	0.1%	1321.08	0.1%	-6%	755.69	0.2%	830.34	0.1%	-9%	354.94	0.2%	392.12	0.1%
	200	999.31	0.1%	980.72	0.1%	2%	985.06	0.2%	1089.81	0.1%	-10%	946.71	0.1%	973.84	0.1%
	500	580.77	0.1%	583.47	0.1%	-0.5%	586.04	0.2%	578.29	0.1%	1%	586.78	0.1%	588.61	0.1%
	1000	552.68	0.2%	553.69	0.1%	-0.2%	559.08	0.2%	552.82	0.2%	1%	565.63	0.1%	568.16	0.1%
	2000	555.89	0.2%	555.85	0.2%	0.0%	557.88	0.2%	556.03	0.2%	0.3%	570.30	0.1%	570.93	0.1%
Lungs	5000	630.22	0.2%	629.19	0.2%	0.2%	630.85	0.2%	639.10	0.2%	-1%	658.76	0.1%	659.46	0.1%
	10000	754.52	0.3%	750.92	0.2%	0.5%	751.75	0.3%	762.02	0.2%	-1%	792.24	0.1%	793.16	0.1%
LLAT		Sitting phantom		Standing phantom		Sitting phantom		Standing phantom		Sitting phantom		Standing phantom			
	Energy (MeV)	$D_{\gamma}\phi$ (pGy cm <sup>2</sup> )	Relative error	$D_{\gamma}\phi$ (pGy cm <sup>2</sup> )	Relative difference (RD)	$D_{\gamma}\phi$ (pGy cm <sup>2</sup> )	Relative error	$D_{\gamma}\phi$ (pGy cm <sup>2</sup> )	Relative difference (RD)	$D_{\gamma}\phi$ (pGy cm <sup>2</sup> )	Relative error	$D_{\gamma}\phi$ (pGy cm <sup>2</sup> )	Relative error		
Extrathoracic region	5	0.0024	4.8%	0.0023	3.7%	6%	26.40	1.3%	26.50	1.0%	-0.4%	0.018	7.0%	0.020	6.2%
	10	0.0104	2.6%	0.0098	1.9%	6%	61.36	1.1%	61.77	0.8%	-1%	0.06	6.7%	0.05	5.2%
	20	0.03	1.7%	0.02	1.5%	3%	993%	0.7%	133.45	0.5%	1%	37.39	0.9%	37.58	0.7%
	30	1.44	1.1%	0.13	1.5%	1%	134.70	0.7%	1867.72	0.2%	0.1%	2088.07	0.2%	2084.69	0.2%
	50	228.05	0.1%	230.32	0.1%	-1%	1868.72	0.2%	1084.08	0.2%	0.1%	1075.13	0.2%	1071.86	0.2%
	100	760.41	0.1%	776.36	0.1%	-2%	1085.46	0.2%	862.45	0.2%	-0.1%	858.84	0.2%	857.97	0.2%
	200	1103.33	0.1%	1091.62	0.1%	1%	862.00	0.2%	568.01	0.2%	0.0%	565.48	0.3%	564.79	0.2%
	500	567.12	0.1%	566.31	0.1%	0.1%	567.89	0.3%	536.10	0.3%	-1%	534.42	0.4%	531.21	0.3%
	1000	533.41	0.1%	532.98	0.1%	0.1%	533.32	0.4%	531.20	0.4%	-1%	531.62	0.4%	530.04	0.3%
	2000	543.28	0.1%	542.35	0.1%	0.2%	528.51	0.5%	602.41	0.5%	-2%	592.63	0.5%	593.70	0.4%
Oral mucosa	5000	630.34	0.1%	629.31	0.1%	0.2%	704.39	0.6%	709.14	0.5%	-1%	703.26	0.6%	705.01	0.5%
	10000	756.95	0.1%	755.83	0.1%	0.1%									

(Continued)

**Table B.4.** (*Continued*)

(Continued)

**Table B.4.** (*Continued*)

LLAT	Sitting phantom			Standing phantom			Sitting phantom			Standing phantom			
	Energy (MeV)	$D_{\gamma}/\phi$ (pGy cm <sup>2</sup> )	Relative error	$D_{\gamma}/\phi$ (pGy cm <sup>2</sup> )									
Stomach	5	10	0.003	8.5%	0.004	6.4%	-15%			0.016	10.3%	0.015	7.8%
	20	0.016	4.3%	0.017	3.2%	-4%			0.040	7.6%	0.039	5.4%	1%
	30	0.042	3.3%	0.041	2.3%	-2%	0.028	12.7%	0.029	6.8%	-2%		
	50	0.20	3.1%	0.22	2.6%	-9%	0.15	14.9%	0.14	8.8%	4%	186.63	0.9%
	100	777.57	0.2%	1193.96	0.1%	-35%	2.22	7.0%	1.92	5.4%	16%	1292.92	0.5%
	150	1278.05	0.1%	1269.12	0.1%	1%	1885.76	0.4%	1858.16	1%	1250.32	0.4%	1244.48
	200	947.20	0.1%	917.82	0.1%	3%	987.38	0.4%	978.37	0.3%	904.24	0.4%	902.48
	500	577.02	0.2%	583.84	0.1%	-1%	571.81	0.5%	564.46	0.3%	576.37	0.5%	578.58
	1000	546.77	0.2%	552.97	0.2%	-1%	538.40	0.6%	535.03	0.4%	547.15	0.6%	546.21
	2000	550.20	0.3%	553.10	0.2%	-1%	549.22	0.7%	539.61	0.5%	548.69	0.7%	542.55
Tonsil	5000	623.32	0.3%	623.55	0.2%	0.0%	618.78	0.8%	615.77	0.6%	614.27	0.8%	617.02
	10000	745.76	0.3%	739.76	0.2%	1%	741.03	0.9%	732.49	0.6%	732.11	1.1%	732.20
LLAT													
5	10	0.010	6.6%	0.008	5.7%	20%			0.009	8.1%	0.007	7.3%	
Uterus	20	0.021	5.4%	0.018	4.6%	16%			0.020	7.0%	0.018	5.6%	14%
	30	0.12	7.3%	0.10	5.9%	26%			0.13	7.0%	0.10	5.0%	24%
	50	1.56	4.1%	1.30	3.5%	20%			1.57	3.6%	1.32	3.0%	18%
	100	2273.53	0.8%	2338.20	0.6%	-3%	877.48	0.3%	525.73	0.3%	718.42	0.3%	106.99
	150	1116.86	0.8%	1117.43	0.6%	-0.1%	1086.49	0.2%	1270.38	0.2%	1114.22	0.3%	1357.86
	200	870.09	0.8%	867.44	0.6%	0.3%	593.96	0.2%	580.12	0.2%	598.22	0.3%	582.76
	500	576.17	1.0%	568.59	0.7%	1%	574.31	0.3%	555.14	0.2%	577.37	0.3%	561.03
	1000	552.83	1.3%	538.19	0.9%	3%	574.28	0.4%	560.78	0.3%	573.30	0.4%	565.03
	2000	543.20	1.5%	531.12	1.1%	2%	650.68	0.4%	646.63	0.3%	648.18	0.4%	644.20
	5000	591.37	1.6%	584.55	1.2%	1%	785.88	0.5%	779.20	0.4%	781.91	0.5%	776.44

(Continued)

**Table B.4.** (*Continued*)

**Table B.5.** Absorbed dose per unit fluence ( $\text{pGy cm}^2$ ) under ROT geometry from monoenergetic protons for UFH/NCI in standing and sitting posture.

ROT	Sitting phantom			Standing phantom			Sitting phantom			Standing phantom			Sitting phantom			Standing phantom		
	Energy (MeV)	$D_{\text{r}}/\phi$ ( $\text{pGy cm}^2$ )	Relative error															
Adrenals	2	5																
	10	0.0039	9.8%	0.0035	9.9%	11%												
	20	0.015	5.0%	0.016	4.7%	-5%												
	30	0.039	5.1%	0.040	3.9%	-3%	0.0392	10.3%	0.0389	10.0%	1%							
	50	3.49	2.6%	2.47	2.7%	41%	0.193	10.4%	0.182	8.3%	6%							
	100	540.54	0.3%	61.483	0.3%	-12%	266.98	1.1%	251.61	1.1%	6%							
	150	1102.64	0.2%	1085.14	0.2%	2%	1448.81	0.4%	1333.10	0.4%	9%							
	200	1074.10	0.2%	1022.12	0.2%	5%	1066.11	0.4%	981.65	0.4%	9%							
	500	630.66	0.2%	601.17	0.2%	5%	638.52	0.5%	591.31	0.5%	8%							
	1000	601.82	0.3%	573.86	0.2%	5%	604.25	0.7%	553.51	0.6%	9%							
Colon	2000	599.55	0.3%	574.67	0.3%	4%	611.13	0.8%	565.42	0.8%	8%							
	5000	677.25	0.3%	647.33	0.3%	5%	681.09	0.9%	633.08	0.9%	8%							
	10000	809.95	0.4%	778.13	0.4%	4%	810.83	0.9%	775.99	1.6%	4%	813.63	1.5%	771.58	1.5%	771.58	1.5%	771.58

(Continued)

**Table B.5.** (*Continued*)

ROT	Sitting phantom			Standing phantom			Sitting phantom			Standing phantom			
	Energy (MeV)	$D_{T/\phi}$ (pGy cm <sup>2</sup> )	Relative error										
Heart	5	2											
	10	0.015	6.7%	0.017	6.1%	-7%	0.019	6.9%	0.018	6.4%	6%	0.0037	9.9%
	20	0.036	5.7%	0.036	4.6%	0%	0.049	5.8%	0.046	5.5%	7%	0.015	4.9%
	30	0.18	5.4%	0.19	6.4%	-4%	129.50	0.6%	125.15	0.6%	3%	0.040	3.7%
	50	399.75	0.4%	391.44	0.4%	2%	964.76	0.3%	779.38	0.3%	24%	2.50	1.5%
	100	1324.11	0.2%	1269.86	0.2%	4%	975.45	0.3%	950.81	0.3%	3%	518.48	0.2%
	150	1048.80	0.2%	1003.09	0.2%	5%	1083.90	0.2%	1014.65	0.2%	7%	1124.59	0.2%
	200	618.27	0.3%	590.76	0.3%	5%	653.72	0.3%	597.55	0.3%	9%	1078.55	0.2%
	500	591.55	0.3%	563.76	0.3%	5%	621.43	0.3%	568.73	0.3%	9%	631.63	0.2%
	1000	594.01	0.4%	566.19	0.4%	5%	622.00	0.4%	569.11	0.4%	9%	604.93	0.2%
Lungs	5000	662.85	0.4%	636.73	0.4%	4%	708.29	0.4%	647.98	0.4%	9%	605.17	0.3%
	10000	794.23	0.5%	763.13	0.5%	4%	841.52	0.5%	767.99	0.5%	10%	680.59	0.2%
	5	2											
	10	0.0035	7.7%	0.0033	7.4%	5%	1.81	9.1%	1.90	8.4%	-5%		
	20	0.017	3.6%	0.017	3.4%	0%	20.97	3.1%	21.53	2.9%	-3%		
Extrathoracic region	30	0.041	2.7%	0.040	2.8%	4%	54.81	2.2%	54.79	2.1%	0%		
	50	5.07	1.4%	4.05	1.4%	25%	390.53	1.0%	388.54	0.9%	1%	12.87	3.2%
	100	981.45	0.2%	960.47	0.2%	2%	1440.99	0.5%	1389.09	0.5%	4%	1895.69	0.5%
	150	1209.63	0.1%	1141.54	0.1%	6%	1201.25	0.5%	1146.66	0.4%	5%	1208.32	0.4%
	200	1046.21	0.1%	978.39	0.1%	7%	916.40	0.5%	875.62	0.4%	5%	929.46	0.5%
	500	625.07	0.1%	586.95	0.1%	6%	590.41	0.6%	567.83	0.6%	4%	605.21	0.6%
	1000	588.03	0.2%	550.76	0.2%	7%	557.93	0.8%	532.11	0.8%	5%	571.07	0.7%
	2000	595.00	0.2%	557.87	0.2%	7%	561.72	1.0%	542.52	1.1%	4%	560.84	0.8%
	5000	677.16	0.2%	636.74	0.2%	6%	625.77	1.1%	618.24	1.1%	1%	633.27	0.9%
	10000	810.24	0.3%	760.58	0.2%	7%	738.75	1.1%	718.76	1.1%	3%	747.89	0.9%
Oral mucosa	5	2											
	10	0.0035	7.7%	0.0033	7.4%	5%	1.81	9.1%	1.90	8.4%	-5%		
	20	0.017	3.6%	0.017	3.4%	0%	20.97	3.1%	21.53	2.9%	-3%		
	30	0.041	2.7%	0.040	2.8%	4%	54.81	2.2%	54.79	2.1%	0%		
	50	5.07	1.4%	4.05	1.4%	25%	390.53	1.0%	388.54	0.9%	1%		
	100	981.45	0.2%	960.47	0.2%	2%	1440.99	0.5%	1389.09	0.5%	4%		
	150	1209.63	0.1%	1141.54	0.1%	6%	1201.25	0.5%	1146.66	0.4%	5%		
	200	1046.21	0.1%	978.39	0.1%	7%	916.40	0.5%	875.62	0.4%	5%		
	500	625.07	0.1%	586.95	0.1%	6%	590.41	0.6%	567.83	0.6%	4%		
	1000	588.03	0.2%	550.76	0.2%	7%	557.93	0.8%	532.11	0.8%	5%		
(Continued)	2												
	10	0.0035	7.7%	0.0033	7.4%	5%	1.81	9.1%	1.90	8.4%	-5%		
	20	0.017	3.6%	0.017	3.4%	0%	20.97	3.1%	21.53	2.9%	-3%		
	30	0.041	2.7%	0.040	2.8%	4%	54.81	2.2%	54.79	2.1%	0%		
	50	5.07	1.4%	4.05	1.4%	25%	390.53	1.0%	388.54	0.9%	1%		
Liver	100	981.45	0.2%	960.47	0.2%	2%	1440.99	0.5%	1389.09	0.5%	4%		
	150	1209.63	0.1%	1141.54	0.1%	6%	1201.25	0.5%	1146.66	0.4%	5%		
	200	1046.21	0.1%	978.39	0.1%	7%	916.40	0.5%	875.62	0.4%	5%		
	500	625.07	0.1%	586.95	0.1%	6%	590.41	0.6%	567.83	0.6%	4%		
	1000	588.03	0.2%	550.76	0.2%	7%	557.93	0.8%	532.11	0.8%	5%		
	2000	595.00	0.2%	557.87	0.2%	7%	561.72	1.0%	542.52	1.1%	4%		
	5000	677.16	0.2%	636.74	0.2%	6%	625.77	1.1%	618.24	1.1%	1%		
	10000	810.24	0.3%	760.58	0.2%	7%	738.75	1.1%	718.76	1.1%	3%		
	5	2											
	10	0.0035	7.7%	0.0033	7.4%	5%	1.81	9.1%	1.90	8.4%	-5%		
	20	0.017	3.6%	0.017	3.4%	0%	20.97	3.1%	21.53	2.9%	-3%		
	30	0.041	2.7%	0.040	2.8%	4%	54.81	2.2%	54.79	2.1%	0%		
	50	5.07	1.4%	4.05	1.4%	25%	390.53	1.0%	388.54	0.9%	1%		
	100	981.45	0.2%	960.47	0.2%	2%	1440.99	0.5%	1389.09	0.5%	4%		
	150	1209.63	0.1%	1141.54	0.1%	6%	1201.25	0.5%	1146.66	0.4%	5%		
	200	1046.21	0.1%	978.39	0.1%	7%	916.40	0.5%	875.62	0.4%	5%		
	500	625.07	0.1%	586.95	0.1%	6%	590.41	0.6%	567.83	0.6%	4%		
	1000	588.03	0.2%	550.76	0.2%	7%	557.93	0.8%	532.11	0.8%	5%		
	2000	595.00	0.2%	557.87	0.2%	7%	561.72	1.0%	542.52	1.1%	4%		
	5000	677.16	0.2%	636.74	0.2%	6%	625.77	1.1%	618.24	1.1%	1%		
	10000	810.24	0.3%	760.58	0.2%	7%	738.75	1.1%	718.76	1.1%	3%		
Oral mucosa	5	2											
	10	0.0035	7.7%	0.0033	7.4%	5%	1.81	9.1%	1.90	8.4%	-5%		
	20	0.017	3.6%	0.017	3.4%	0%	20.97	3.1%	21.53	2.9%	-3%		
	30	0.041	2.7%	0.040	2.8%	4%	54.81	2.2%	54.79	2.1%	0%		
	50	5.07	1.4%	4.05	1.4%	25%	390.53	1.0%	388.54	0.9%	1%		
	100	981.45	0.2%	960.47	0.2%	2%	1440.99	0.5%	1389.09	0.5%	4%		
	150	1209.63	0.1%	1141.54	0.1%	6%	1201.25	0.5%	1146.66	0.4%	5%		
	200	1046.21	0.1%	978.39	0.1%	7%	916.40	0.5%	875.62	0.4%	5%		
	500	625.07	0.1%	586.95	0.1%	6%	590.41	0.6%	567.83	0.6%	4%		
	1000	588.03	0.2%	550.76	0.2%	7%	557.93	0.8%	532.11	0.8%	5%		
Lungs	5	2											
	10	0.0035	7.7%	0.0033	7.4%	5%	1.81	9.1%	1.90	8.4%	-5%		
	20	0.017	3.6%	0.017	3.4%	0%	20.97	3.1%	21.53	2.9%	-3%		
	30	0.041	2.7%	0.040	2.8%	4%	54.81	2.2%	54.79	2.1%	0%		
	50	5.07	1.4%	4.05	1.4%	25%	390.53	1.0%	388.54	0.9%	1%		
	100	981.45	0.2%	960.47	0.2%	2%	1440.99	0.5%	1389.09	0.5%	4%		
	150	1209.63	0.1%	1141.54	0.1%	6%	1201.25	0.5%	1146.66	0.4%	5%		
	200	1046.21	0.1%	978.39	0.1%	7%	916.40	0.5%	875.62	0.4%	5%		
	500	625.07	0.1%	586.95	0.1%	6%	590.41	0.6%	567.83	0.6%	4%		
	1000	588.03	0.2%	550.76	0.2%	7%	557.93	0.8%	532.11	0.8%	5%		
Extrathoracic region	5	2											
	10	0.0035	7.7%	0.0033	7.4%	5%	1.81	9.1%	1.90	8.4%	-5%		
	20	0.017	3.6%	0.017	3.4%	0%	20.97	3.1%	21.53	2.9%	-3%		
	30	0.041	2.7%	0.040	2.8%	4%	54.81	2.2%	54.79	2.1%	0%		
	50	5.07	1.4%	4.05	1.4%	25%	390.53	1.0%	388.54	0.9%	1%		
	100	981.45	0.2%	960.47	0.2%	2%	1440.99	0.5%	1389.09	0.5%	4%		
	150	1209.63	0.1%	1141.54	0.1%	6%	1201.25	0.5%	1146.66	0.4%	5%		
	200	1046.21	0.1%	978.39	0.1%	7%</							

**Table B.5.** (*Continued*)

ROT	Sitting phantom			Standing phantom			Sitting phantom			Standing phantom														
	Energy (MeV)	$D_{\gamma}/\phi$ (pGy cm <sup>2</sup> )	Relative error	$D_{\gamma}/\phi$ (pGy cm <sup>2</sup> )																				
Ovaries	5	10																						
	10	1265.66	1.0%	1234.00	0.9%	3%	0.016	9.7%	0.018	10.2%	-10%	0.49	11.0%	0.62	9.2%	-21%								
	20	1145.19	0.8%	1057.83	0.8%	8%	0.035	7.9%	0.035	8.8%	0%	35.43	1.4%	32.15	1.4%	10%								
	30	644.51	1.0%	601.31	1.0%	7%	0.197	6.7%	0.203	8.9%	-3%	218.77	0.8%	202.53	0.8%	8%								
	50	607.33	1.3%	572.15	1.3%	6%	268.07	0.8%	235.01	0.8%	14%	676.89	0.6%	645.25	0.6%	5%								
	100	611.32	1.6%	581.03	1.4%	5%	1382.71	0.4%	1293.81	0.3%	7%	1262.88	0.4%	1223.25	0.4%	3%								
	200	686.20	1.6%	655.04	1.6%	5%	1089.13	0.4%	1030.79	0.4%	6%	1237.77	0.4%	1186.21	0.4%	4%								
	500	835.54	1.7%	790.57	1.6%	6%	647.75	0.4%	604.01	0.4%	7%	928.88	0.4%	887.33	0.4%	5%								
	1000						620.58	0.5%	575.57	0.5%	8%	598.36	0.5%	570.44	0.4%	5%								
	10000						621.48	0.6%	585.45	0.6%	6%	558.64	0.6%	532.39	0.6%	5%								
Small intestine	5	10																						
	10	0.0034	9.8%	0.0035	9.5%	-1%	304.52	0.0%	311.49	0.0%	-2%	752.85	0.0%	769.44	0.0%	-2%								
	20	0.013	4.6%	0.015	4.5%	-11%	1458.91	0.0%	1487.11	0.0%	-2%	2093.17	0.0%	2121.46	0.0%	-1%								
	30	0.035	3.4%	0.036	3.3%	-3%	1602.71	0.0%	1634.51	0.0%	-2%	1152.24	0.0%	1198.49	0.0%	-4%								
	50	1.20	2.8%	2.73	1.9%	-56%	1002.05	0.1%	1061.98	0.0%	-6%	953.39	0.0%	995.85	0.0%	-4%								
	100	332.92	0.3%	384.79	0.2%	-13%	1240.62	0.1%	1152.48	0.0%	-1%	926.51	0.0%	919.56	0.0%	-1%								
	150	1288.93	0.2%	1017.69	0.1%	5%	1070.86	0.2%	602.80	0.2%	5%	578.48	0.1%	568.11	0.0%	2%								
	200	635.74	0.2%	645.81	0.3%	5%	573.02	0.2%	532.17	0.1%	521.88	0.1%	524.08	0.1%	512.52	0.1%	511.12	0.1%	505.92	0.1%	503.66	0.1%		
	500	606.10	0.2%	574.27	0.2%	6%	606.25	0.3%	645.81	0.3%	6%	708.80	0.1%	688.34	0.1%	3%	699.95	0.6%	649.57	0.6%	677.51	0.6%	610.72	0.6%
	10000	816.45	0.3%	773.66	0.3%	6%						831.07	0.6%	778.73	0.7%	7%								

(Continued)

**Table B.5.** (*Continued*)

ROT	Sitting phantom			Standing phantom			Sitting phantom			Standing phantom			
	Energy (MeV)	$D_{T/\Phi}$ (pGy cm <sup>2</sup> )	Relative error										
Stomach	5	20	0.018	7.7%	0.017	7.2%	7%						
	10	0.039	5.7%	0.038	6.4%	2%							
	20	0.21	8.1%	0.19	6.1%	11%							
	30	670.09	0.4%	636.18	0.4%	5%	804.59	1.0%	776.21	0.9%	4%	486.58	1.2%
	50	1121.99	0.3%	1097.57	0.3%	2%	1568.42	0.7%	1474.80	0.6%	6%	999.93	0.9%
	100	1043.74	0.3%	1006.90	0.3%	4%	1015.61	0.6%	950.24	0.6%	7%	1328.69	0.6%
	200	628.69	0.3%	603.47	0.3%	4%	612.87	0.8%	572.20	0.7%	7%	935.85	0.6%
	500	596.57	0.4%	575.87	0.4%	4%	574.88	1.0%	542.66	1.0%	6%	593.10	0.8%
	1000	600.65	0.5%	577.87	0.5%	4%	578.11	1.2%	540.82	1.2%	7%	559.02	1.1%
	2000	676.03	0.5%	648.56	0.5%	4%	650.03	1.4%	607.03	1.2%	7%	556.81	1.3%
Tonsil	5	809.40	0.6%	771.41	0.5%	5%	783.33	1.4%	731.69	1.3%	7%	725.34	1.5%
	10												
	20												
	30												
	50												
	100												
	150												
	200												
	500												
	1000												

(Continued)

**Table B.5.** (*Continued*)

ROT	Sitting phantom			Standing phantom			Sitting phantom			Standing phantom				
	Energy (MeV)	$D_{T/\phi}$ (pGy cm <sup>2</sup> )	Relative error											
<b>Muscle</b>														
2	0.017	1.4%	0.017	1.3%	0%	0.05	4.9%	0.06	4.1%	-19%	0.019	5.5%	0.024	4.5%
5	0.258	0.6%	0.261	0.5%	-1%	0.10	0.7%	0.08	0.6%	1%	0.20	0.9%	0.18	0.9%
10	1.81	0.3%	1.81	0.3%	0%	3%	-3%	4.10	0.7%	-2%	14.17	0.4%	13.17	0.3%
20	28.86	0.1%	29.70	0.1%	-4%	39.58	0.3%	40.47	0.3%	-1%	147.13	0.2%	139.61	0.2%
30	99.13	0.1%	103.00	0.1%	-10%	288.64	0.1%	291.32	0.1%	-10%				
50	335.07	0.1%	371.43	0.0%	-12%	1005.27	0.1%	1121.77	0.1%	-10%	700.82	0.1%	684.57	0.1%
100	882.19	0.0%	998.40	0.0%	-4%	1062.84	0.0%	1119.61	0.1%	-5%	1101.14	0.1%	1085.29	0.1%
150	1034.04	0.0%	1081.70	0.0%	4%	964.75	0.0%	960.47	0.1%	2%	1076.46	0.1%	1003.08	0.1%
200	1000.45	0.0%	988.79	0.0%	4%	601.37	0.1%	581.48	0.1%	3%	634.28	0.1%	593.44	0.1%
500	610.84	0.1%	554.16	0.1%	4%	568.69	0.1%	549.88	0.1%	3%	605.34	0.1%	566.57	0.1%
1000	575.99	0.1%	553.79	0.1%	4%	565.82	0.1%	545.28	0.1%	4%	602.47	0.1%	563.61	0.1%
2000	576.57	0.1%	631.50	0.1%	5%	636.76	0.1%	610.00	0.1%	4%	673.98	0.1%	627.97	0.1%
5000	661.16	0.1%	749.38	0.1%	5%	763.43	0.1%	728.82	0.1%	5%	809.50	0.2%	755.10	0.2%
10000	785.79	0.1%												

**Table B.6.** Absorbed dose per unit fluence ( $\text{pGy cm}^2$ ) under ISO geometry from monoenergetic protons for UFH/NCI in standing and sitting posture.

ISO	Sitting phantom		Standing phantom		Sitting phantom		Standing phantom		Sitting phantom		Standing phantom	
	Energy (MeV)	$D_{\gamma}/\phi$ ( $\text{pGy cm}^2$ )	Relative error	$D_{\gamma}/\phi$ ( $\text{pGy cm}^2$ )	Relative error	Relative difference (RD)	$D_{\gamma}/\phi$ ( $\text{pGy cm}^2$ )	Relative error	$D_{\gamma}/\phi$ ( $\text{pGy cm}^2$ )	Relative difference (RD)	$D_{\gamma}/\phi$ ( $\text{pGy cm}^2$ )	Relative error
2	5											
10	0.002	7.2%	0.003	8.7%	-12%		0.013	8.4%	0.009	10.7%	45%	
20	0.013	3.8%	0.012	4.0%	8%		0.028	6.7%	0.029	6.9%	-2%	
30	0.029	2.7%	0.030	3.4%	-3%		0.15	8.2%	0.14	5.1%	2%	
50	1.45	2.3%	0.93	3.0%	56%		215.35	0.8%	220.78	1.0%	-2%	
100	330.60	0.2%	389.11	0.2%	-15%		1087.19	0.3%	1076.62	0.4%	1%	
150	756.52	0.1%	820.85	0.2%	-8%		938.17	0.1%	941.79	0.3%	-0.4%	
200	939.40	0.1%	913.83	0.1%	3%		585.98	0.3%	582.73	0.4%	1%	
500	589.97	0.1%	585.54	0.1%	1%		558.13	0.5%	553.40	0.5%	1%	
1000	565.37	0.2%	559.51	0.2%	1%		561.11	0.5%	557.14	0.6%	0.6%	
2000	568.89	0.2%	562.12	0.2%	1%		638.99	0.6%	638.99	0.8%	0.0%	
5000	653.41	0.2%	647.00	0.2%	1%		767.22	0.7%	768.89	0.8%	-0.2%	
10000	784.18	0.2%	775.36	0.3%	1%							
Adrenals												
10	0.002	7.2%	0.003	8.7%	-12%		0.013	8.4%	0.009	10.7%	45%	
20	0.013	3.8%	0.012	4.0%	8%		0.028	6.7%	0.029	6.9%	-2%	
30	0.029	2.7%	0.030	3.4%	-3%		0.15	8.2%	0.14	5.1%	2%	
50	1.45	2.3%	0.93	3.0%	56%		215.35	0.8%	220.78	1.0%	-2%	
100	330.60	0.2%	389.11	0.2%	-15%		1087.19	0.3%	1076.62	0.4%	1%	
150	756.52	0.1%	820.85	0.2%	-8%		938.17	0.1%	941.79	0.3%	-0.4%	
200	939.40	0.1%	913.83	0.1%	3%		585.98	0.3%	582.73	0.4%	1%	
500	589.97	0.1%	585.54	0.1%	1%		558.13	0.5%	553.40	0.5%	1%	
1000	565.37	0.2%	559.51	0.2%	1%		561.11	0.5%	557.14	0.6%	0.6%	
2000	568.89	0.2%	562.12	0.2%	1%		638.99	0.6%	638.99	0.8%	0.0%	
5000	653.41	0.2%	647.00	0.2%	1%		767.22	0.7%	768.89	0.8%	-0.2%	
10000	784.18	0.2%	775.36	0.3%	1%							
Colon												
10	0.002	7.2%	0.003	8.7%	-12%		0.013	8.4%	0.009	10.7%	45%	
20	0.013	3.8%	0.012	4.0%	8%		0.028	6.7%	0.029	6.9%	-2%	
30	0.029	2.7%	0.030	3.4%	-3%		0.15	8.2%	0.14	5.1%	2%	
50	1.45	2.3%	0.93	3.0%	56%		215.35	0.8%	220.78	1.0%	-2%	
100	330.60	0.2%	389.11	0.2%	-15%		1087.19	0.3%	1076.62	0.4%	1%	
150	756.52	0.1%	820.85	0.2%	-8%		938.17	0.1%	941.79	0.3%	-0.4%	
200	939.40	0.1%	913.83	0.1%	3%		585.98	0.3%	582.73	0.4%	1%	
500	589.97	0.1%	585.54	0.1%	1%		558.13	0.5%	553.40	0.5%	1%	
1000	565.37	0.2%	559.51	0.2%	1%		561.11	0.5%	557.14	0.6%	0.6%	
2000	568.89	0.2%	562.12	0.2%	1%		638.99	0.6%	638.99	0.8%	0.0%	
5000	653.41	0.2%	647.00	0.2%	1%		767.22	0.7%	768.89	0.8%	-0.2%	
10000	784.18	0.2%	775.36	0.3%	1%							
Oesophagus												
10	0.002	7.2%	0.003	8.7%	-12%		0.013	8.4%	0.009	10.7%	45%	
20	0.013	3.8%	0.012	4.0%	8%		0.028	6.7%	0.029	6.9%	-2%	
30	0.029	2.7%	0.030	3.4%	-3%		0.15	8.2%	0.14	5.1%	2%	
50	1.45	2.3%	0.93	3.0%	56%		215.35	0.8%	220.78	1.0%	-2%	
100	330.60	0.2%	389.11	0.2%	-15%		1087.19	0.3%	1076.62	0.4%	1%	
150	756.52	0.1%	820.85	0.2%	-8%		938.17	0.1%	941.79	0.3%	-0.4%	
200	939.40	0.1%	913.83	0.1%	3%		585.98	0.3%	582.73	0.4%	1%	
500	589.97	0.1%	585.54	0.1%	1%		558.13	0.5%	553.40	0.5%	1%	
1000	565.37	0.2%	559.51	0.2%	1%		561.11	0.5%	557.14	0.6%	0.6%	
2000	568.89	0.2%	562.12	0.2%	1%		638.99	0.6%	638.99	0.8%	0.0%	
5000	653.41	0.2%	647.00	0.2%	1%		767.22	0.7%	768.89	0.8%	-0.2%	
10000	784.18	0.2%	775.36	0.3%	1%							
Gall bladder												
10	0.002	7.2%	0.003	8.7%	-12%		0.013	8.4%	0.009	10.7%	45%	
20	0.013	3.8%	0.012	4.0%	8%		0.028	6.7%	0.029	6.9%	-2%	
30	0.029	2.7%	0.030	3.4%	-3%		0.15	8.2%	0.14	5.1%	2%	
50	1.45	2.3%	0.93	3.0%	56%		215.35	0.8%	220.78	1.0%	-2%	
100	330.60	0.2%	389.11	0.2%	-15%		1087.19	0.3%	1076.62	0.4%	1%	
150	756.52	0.1%	820.85	0.2%	-8%		938.17	0.1%	941.79	0.3%	-0.4%	
200	939.40	0.1%	913.83	0.1%	3%		585.98	0.3%	582.73	0.4%	1%	
500	589.97	0.1%	585.54	0.1%	1%		558.13	0.5%	553.40	0.5%	1%	
1000	565.37	0.2%	559.51	0.2%	1%		561.11	0.5%	557.14	0.6%	0.6%	
2000	568.89	0.2%	562.12	0.2%	1%		638.99	0.6%	638.99	0.8%	0.0%	
5000	653.41	0.2%	647.00	0.2%	1%		767.22	0.7%	768.89	0.8%	-0.2%	
10000	784.18	0.2%	775.36	0.3%	1%							
Sitting phantom												
10	0.002	7.2%	0.003	8.7%	-12%		0.013	8.4%	0.009	10.7%	45%	
20	0.013	3.8%	0.012	4.0%	8%		0.028	6.7%	0.029	6.9%	-2%	
30	0.029	2.7%	0.030	3.4%	-3%		0.15	8.2%	0.14	5.1%	2%	
50	1.45	2.3%	0.93	3.0%	56%		215.35	0.8%	220.78	1.0%	-2%	
100	330.60	0.2%	389.11	0.2%	-15%		1087.19	0.3%	1076.62	0.4%	1%	
150	756.52	0.1%	820.85	0.2%	-8%		938.17	0.1%	941.79	0.3%	-0.4%	
200	939.40	0.1%	913.83	0.1%	3%		585.98	0.3%	582.73	0.4%	1%	
500	589.97	0.1%	585.54	0.1%	1%		558.13	0.5%	553.40	0.5%	1%	
1000	565.37	0.2%	559.51	0.2%	1%		561.11	0.5%	557.14	0.6%	0.6%	
2000	568.89	0.2%	562.12	0.2%	1%		638.99	0.6%	638.99	0.8%	0.0%	
5000	653.41	0.2%	647.00	0.2%	1%		767.22	0.7%	768.89	0.8%	-0.2%	
10000	784.18	0.2%	775.36	0.3%	1%							
Standing phantom												
10	0.002	7.2%	0.003	8.7%	-12%		0.013	8.4%	0.009	10.7%	45%	
20	0.013	3.8%	0.012	4.0%	8%		0.028	6.7%	0.029	6.9%	-2%	
30	0.029	2.7%	0.030	3.4%	-3%		0.15	8.2%	0.14	5.1%	2%	
50	1.45	2.3%	0.93	3.0%	56%		215.35	0.8%	220.78	1.0%	-2%	
100	330.60	0.2%	389.11	0.2%	-15%		1087.19	0.3%	1076.62	0.4%	1%	
150	756.52	0.1%	820.85	0.2%	-8%		938.17	0.1%	941.79	0.3%	-0.4%	
200	939.40	0.1%	913.83	0.1%	3%		585.98	0.3%	582.73	0.4%	1%	
500	589.97	0.1%	585.54	0.1%	1%		558.13	0.5%	553.40	0.5%	1%	
1000	565.37	0.2%	559.51	0.2%	1%		561.11	0.5%	557.14	0.6%	0.6%	
2000	568.89	0.2%	562.12	0.2%	1%		638.99	0.6%	638.99	0.8%	0.0%	
5000	653.41	0.2%	647.00	0.2%	1%		767.22	0.7%	768.89	0.8%	-0.2%	
10000	784.18	0.2%	775.36	0.3%	1%							

(Continued)

**Table B.6.** (Continued)

ISO	Sitting phantom			Standing phantom			Sitting phantom			Standing phantom								
	Energy (MeV)	$D_{T/\Phi}$ (pGy cm <sup>2</sup> )	Relative error															
Heart	5	10	0.0118	4.9%	0.0115	5.7%	2%	0.013	5.1%	0.012	6.1%	12%	0.003	7.6%	0.002	8.1%	8%	
	20	0.030	4.8%	0.028	4.2%	11%	0.034	4.2%	0.033	4.3%	1%	0.029	2.7%	0.012	3.4%	4.2%	7%	
	50	0.14	4.0%	0.15	4.5%	-2%	61.26	0.5%	61.40	0.6%	0%	1.07	1.4%	0.53	2.0%	3%	100%	
	100	306.60	0.3%	306.34	0.3%	0.1%	665.13	0.2%	606.29	0.3%	10%	284.69	0.2%	289.39	0.2%	-2%	-2%	
	150	1010.38	0.2%	1019.93	0.2%	-1%	654.30	0.2%	682.21	0.2%	-4%	830.39	0.1%	848.38	0.1%	-2%	-2%	
	200	936.97	0.2%	943.89	0.2%	-1%	862.81	0.2%	898.16	0.2%	-4%	940.84	0.1%	959.15	0.1%	-2%	-2%	
	500	585.97	0.2%	584.33	0.2%	0.3%	577.43	0.2%	576.36	0.2%	0.2%	586.42	0.1%	585.55	0.1%	0.1%	0.1%	
	1000	559.32	0.2%	554.66	0.2%	1%	550.70	0.2%	549.59	0.3%	0.2%	560.47	0.1%	559.25	0.2%	0.2%	0.2%	
	2000	562.74	0.3%	557.37	0.3%	1%	554.35	0.3%	550.64	0.3%	1%	565.62	0.2%	563.38	0.2%	0.4%	0.4%	
	5000	643.83	0.3%	639.81	0.3%	1%	639.85	0.3%	637.07	0.3%	0.4%	647.27	0.2%	644.18	0.2%	0.5%	0.5%	
	10000	767.71	0.3%	765.52	0.3%	0.3%	764.09	0.3%	761.07	0.3%	0.4%	777.20	0.2%	774.55	0.2%	0.3%	0.3%	
ISO		Sitting phantom			Standing phantom			Sitting phantom			Standing phantom							
Lungs	5	10	0.0027	5.4%	0.0028	6.3%	-4%	1.56	6.5%	1.44	8.0%	8%	6.39	2.8%	6.50	3.3%	-2%	-2%
	20	0.012	2.6%	0.013	3.0%	-3%	15.11	2.6%	15.73	3.0%	-4%	1075.65	0.4%	1070.72	0.5%	0.5%	0.5%	
	30	0.031	2.0%	0.030	2.4%	5%	51.66	1.5%	52.70	1.8%	-2%	1015.24	0.3%	1006.72	0.4%	1%	1%	
	50	2.33	1.2%	2.02	1.5%	1.5%	201.62	0.8%	208.92	1.0%	-3%	891.66	0.3%	889.65	0.4%	0.2%	0.2%	
	100	753.70	0.1%	757.24	0.1%	-0.5%	892.99	0.4%	893.74	0.5%	-0.1%	567.46	0.4%	563.40	0.4%	1%	1%	
	150	1020.39	0.1%	1024.27	0.1%	-0.4%	961.63	0.4%	962.71	0.4%	-0.1%	532.56	0.5%	531.69	0.6%	0.2%	0.2%	
	200	901.50	0.1%	907.80	0.1%	-1%	899.49	0.4%	898.70	0.4%	0.1%	521.22	0.7%	537.77	0.6%	534.68	0.7%	
	500	575.00	0.1%	572.55	0.1%	0.4%	556.14	0.4%	555.73	0.5%	0.1%	526.08	0.8%	510.29	0.6%	617.35	0.7%	
	1000	540.67	0.1%	537.45	0.1%	1%	521.77	0.5%	521.22	0.7%	0.1%	507.55	0.9%	507.55	0.7%	-1%	-1%	
	2000	548.82	0.1%	543.99	0.2%	1%	527.65	0.7%	526.08	0.8%	0.3%	510.29	0.8%	510.29	0.7%	617.35	0.7%	
	5000	633.72	0.2%	630.18	0.2%	1%	600.31	0.7%	607.59	0.8%	-1%	593.20	0.9%	593.20	0.7%	-1%	-1%	
	10000	761.02	0.2%	754.50	0.2%	1%	717.46	0.8%	720.82	0.9%	-0.5%	732.20	0.7%	725.52	0.7%	1%	1%	

(Continued)

**Table B.6.** (Continued)

ISO	Sitting phantom			Standing phantom			Sitting phantom			Standing phantom						
	Energy (MeV)	$D_{T/\Phi}$ (pGy cm <sup>2</sup> )	Relative error													
5	10	0.00280	6.9%	0.00277	7.9%	0.011	7.9%	0.011	8.7%	-2%	0.88	5.5%	0.87	6.4%	1%	
10	20	0.0118	3.4%	0.0116	3.7%	0.026	5.3%	0.025	6.0%	2%	18.45	1.4%	18.04	1.7%	2%	
20	30	0.027	2.4%	0.029	2.6%	0.15	7.1%	0.13	7.0%	16%	128.65	0.7%	127.91	0.9%	1%	
30	50	0.117	7.7%	0.123	14.9%	0.026	5.3%	0.025	6.0%	2%	444.80	0.5%	448.37	0.6%	-1%	
50	100	1.56	10.6%	3.28	8.4%	0.15	7.1%	0.13	7.0%	16%	Saltvary glams					
100	150	973.08	0.7%	933.40	0.8%	122.73	0.7%	105.18	0.9%	17%	867.27	0.3%	869.63	0.4%	-0.3%	
150	200	1000.37	0.6%	969.49	0.6%	808.26	0.3%	817.17	0.3%	-1%	1023.29	0.3%	1020.33	0.3%	0.3%	
200	500	592.03	0.6%	596.90	0.7%	956.92	0.3%	997.89	0.3%	-4%	872.62	0.3%	872.28	0.3%	0.0%	
500	1000	568.38	0.8%	566.89	0.9%	594.82	0.3%	592.30	0.3%	0.4%	558.63	0.3%	559.10	0.4%	-0.1%	
1000	2000	570.02	1.0%	562.98	1.0%	570.69	0.3%	567.38	0.4%	1%	525.50	0.4%	524.56	0.5%	0.2%	
2000	5000	655.83	1.4%	651.89	1.1%	654.43	0.4%	655.97	0.4%	-0.2%	525.06	0.5%	521.73	0.6%	1%	
5000	10000	785.26	1.3%	771.78	1.2%	786.16	0.4%	785.20	0.5%	0.1%	600.69	0.5%	602.24	0.6%	-0.3%	
10000	ISO	Sitting phantom	Standing phantom			Sitting phantom	Standing phantom			Sitting phantom	Standing phantom					
2	5	10	0.00280	6.9%	0.00277	7.9%	0.026	5.3%	0.025	6.0%	2%	242.36	0.0%	238.73	0.0%	2%
10	20	30	50	100	150	200	500	1000	1500	2000	5000	10000	ISO	Spleen	Spleen	
5	10	20	30	50	100	150	200	500	1000	1500	2000	5000	10000	ISO	Spleen	
10	20	30	50	100	150	200	500	1000	1500	2000	5000	10000	ISO	Spleen	Spleen	
20	30	50	100	150	200	500	1000	1500	2000	5000	10000	ISO	Spleen	Spleen	Spleen	
30	50	100	150	200	500	1000	1500	2000	5000	10000	ISO	Spleen	Spleen	Spleen	Spleen	
50	100	150	200	500	1000	1500	2000	5000	10000	ISO	Spleen	Spleen	Spleen	Spleen	Spleen	
100	150	200	500	1000	1500	2000	5000	10000	ISO	Spleen	Spleen	Spleen	Spleen	Spleen	Spleen	
150	200	500	1000	1500	2000	5000	10000	ISO	Spleen	Spleen	Spleen	Spleen	Spleen	Spleen	Spleen	
200	500	1000	1500	2000	5000	10000	ISO	Spleen	Spleen	Spleen	Spleen	Spleen	Spleen	Spleen	Spleen	
500	1000	1500	2000	5000	10000	ISO	Spleen	Spleen	Spleen	Spleen	Spleen	Spleen	Spleen	Spleen	Spleen	
1000	1500	2000	5000	10000	ISO	Spleen	Spleen	Spleen	Spleen	Spleen	Spleen	Spleen	Spleen	Spleen	Spleen	
1500	2000	5000	10000	ISO	Spleen	Spleen	Spleen	Spleen	Spleen	Spleen	Spleen	Spleen	Spleen	Spleen	Spleen	
2000	5000	10000	ISO	Spleen	Spleen	Spleen	Spleen									
5000	10000	ISO	Spleen	Spleen	Spleen	Spleen	Spleen									
10000	ISO	Spleen	Spleen	Spleen	Spleen											

(Continued)

**Table B.6.** (*Continued*)

ISO	Sitting phantom			Standing phantom			Sitting phantom			Standing phantom				
	Energy (MeV)	$D_{\gamma}/\Phi$ (pGy cm <sup>2</sup> )	Relative error											
Stomach	2	5												
	10	0.01	5.7%	0.01	7.2%	-7%	0.03	10.0%	0.03	11.9%	26%	1.24	9.9%	
	20	0.03	4.1%	0.03	4.6%	5%	0.03	10.0%	0.03	11.9%	26%	297.39	1.1%	
	30	0.16	5.9%	0.14	4.9%	12%	0.13	10.0%	0.13	11.9%	26%	305.90	1.2%	
	50	331.85	0.4%	361.02	0.4%	-8%	613.94	0.7%	610.67	0.8%	1%	730.90	0.7%	
	100	845.56	0.2%	851.98	0.3%	-1%	1119.43	0.5%	1111.09	0.6%	1%	933.03	0.5%	
	150	933.86	0.2%	954.48	0.2%	-2%	901.65	0.5%	905.16	0.5%	0%	945.02	0.5%	
	200	590.42	0.2%	586.53	0.2%	1%	586.16	0.5%	570.88	0.6%	3%	564.17	0.6%	
	500	1000	0.3%	561.41	0.3%	1%	546.51	0.7%	547.75	0.8%	0%	530.48	0.7%	
	10000	564.88	0.3%	563.81	0.4%	1%	549.11	0.8%	545.02	0.9%	1%	533.34	0.9%	
Tonsil	2	5												
	10	0.01	5.7%	0.01	7.2%	-7%	0.03	10.0%	0.03	11.9%	26%	297.39	1.1%	
	20	0.03	4.1%	0.03	4.6%	5%	0.03	10.0%	0.03	11.9%	26%	305.90	1.2%	
	30	0.16	5.9%	0.14	4.9%	12%	0.13	10.0%	0.13	11.9%	26%	742.25	0.8%	
	50	953.89	1.4%	952.68	1.6%	0%	151.20	0.8%	359.26	0.6%	-12%	0.012	8.3%	
	100	1154.38	0.9%	1125.08	1.1%	3%	801.59	0.3%	736.15	0.4%	-14%	0.026	7.8%	
	150	883.53	0.9%	858.05	1.0%	3%	994.48	0.2%	978.61	0.3%	-18%	0.12	6.8%	
	200	580.40	1.1%	564.53	1.3%	3%	589.89	0.3%	584.67	0.3%	-58%	0.16	1.3%	
	500	1000	545.62	1.6%	523.19	1.5%	4%	568.29	0.4%	563.24	0.4%	0.4%	66.08	0.4%
	10000	538.75	1.7%	542.46	2.3%	-1%	573.33	0.5%	565.46	0.5%	1%	900.68	0.4%	
(Continued)	5000	608.55	2.0%	601.19	2.3%	1%	651.11	0.5%	651.13	0.6%	-1%	985.58	0.3%	
	100000	739.18	2.1%	697.87	2.3%	6%	782.56	0.6%	770.21	0.6%	-1%	594.31	0.3%	

**Table B.6.** (*Continued*)

## References

- Bozkurt A and Xu X G 2004 Fluence-to-dose conversion coefficients for monoenergetic proton beams based on the VIP-man anatomical model *Radiat. Prot. Dosim.* **112** 219–35
- Briesmeister J F 1997 *MCNP—A General Monte Carlo N-Particle Transport Code, Version 4B Report No. LA-12625-M* (Los Alamos, NM: Los Alamos National Laboratory)
- Briesmeister J F 2000 *MCNP—A general Monte Carlo N-Particle Transport Code Report LA-13709-M* (Los Almos, NM: Los Alamos National laboratory)
- ICRP 2007 The 2007 Recommendations of the International Commission on Radiological Protection. ICRP Publication 103 *Ann. ICRP* **37** (2–4) (Oxford: Pergamon)
- ICRP 2010 Conversion Coefficients for Radiological Protection Quantities for External Radiation Exposures. ICRP Publication 116 *Ann. ICRP* **40** (2–5) (Amsterdam: Elsevier)
- Kramer R, Khouri H J, Vieira J W, Loureiro E C M, Lima V J M, Lima F R A and Hoff G 2004 All about FAX: a Female Adult voxel phantom for Monte Carlo calculation in radiation protection dosimetry *Phys. Med. Biol.* **49** 5203–16
- Lee C, Lodwick D, Hasenauer D, Williams J L, Lee C and Bolch W E 2007 Hybrid computational phantoms of the male and female newborn patient: NURBS-based whole-body models *Phys. Med. Biol.* **52** 3309–33
- Lee C, Lodwick D, Hurtado J, Pafundi D, Williams J L and Bolch W E 2010 The UF family of reference hybrid phantoms for computational radiation dosimetry *Phys. Med. Biol.* **55** 339–63
- Pelowitz D B 2011 *MCNPX User's Manual Version 2.7.0* LA-CP-11-00438 (Los Alamos: Los Alamos National Laboratory)
- Piegl L 1991 On NURBS: a survey *IEEE Comput. Graph. Appl.* **11** 55–71
- Sato T, Endo A, Zankl M, Petoussi-Henss N and Niita K 2009 Fluence-to-dose conversion coefficients for neutrons and protons calculated using the PHITS code and ICRP/ICRU adult reference computational phantoms *Phys. Med. Biol.* **54** 1997–2014
- Townsend L W 2001 Radiation exposures of aircrew in high altitude flight *J. Radiol. Prot.* **21** 5–8
- Reitz G 1993 Radiation environment in the stratosphere *Radiat. Prot. Dosim.* **48** 5–20
- Xu X G 2010 Computational phantoms for radiation dosimetry: a 40 year history of evolution *Handbook of Anatomical Models for Radiation Dosimetry* ed X G Xu and K F Eckerman (Boca Raton, FL: Taylor & Francis)
- Zhang G, Liu Q, Zeng S and Luo Q 2008 Organ dose calculations by Monte Carlo modeling of the updated VCH adult male phantom against idealized external proton exposure *Phys. Med. Biol.* **53** 3697–722